Energy, Mines and Resources Canada
Earth Physics Branch
1 Observatory Crescent
Ottawa Canada
K1A 0Y3

Énergie, Mines et Ressources Canada
Direction de la physique du globe
1 Place de l'Observatoire
Ottawa Canada
K1A 0Y3

Geothermal Service of Canada

Service géothermique du Canada

INVESTIGATION OF THERMALLY ACTUATED WATER MIGRATION IN FROZEN SOILS

P.J. Williams and E. Perfect
Geotechnical Science Laboratories, Carleton University

Earth Physics Branch Open File Number 80-16

Ottawa, Canada, 1980

78 p.

Price/Prix: $22.50

Abstract

The report describes the basic theory behind a newly constructed freezing cell parameter and describes experiments illustrating the importance of temperature-induced water migration in saturated frozen soils.

Résumé

Ce rapport décrit la théorie fondamentale derrière un perméamètre à cellule de congélation tout récemment construit. Il décrit également les essais qui démontrent l'importance de la migration d'eau induite par les gradients thermiques dans les sols saturés gelés.

FINAL REPORT

INVESTIGATION OF THERMALLY ACTUATED WATER MIGRATION IN FROZEN SOILS

to the

Department of Energy, Mines and Resources
Earth Physics Branch

by

P.J. WILLIAMS
Principal Investigator

and

E. PERFECT
Research Assistant

Geotechnical Science Laboratories
Department of Geography
Carleton University
Ottawa, Ontario
KIS 5B6

DSS File No. 05SU-23235-9-0484
Contract Serial No. 05U79-00049

April, 1980

TABLE OF CONTENTS

TABLE OF CONTENTS CONTINUED

LIST OF FIGURES AND TABLES

LIST OF FIGURES AND TABLES CONTINUED

I INTRODUCTION

This final report presents the basic theory behind, and findings from freezing experiments carried out between April, 1979 and March, 1980 under the terms of contract no. 05SU-23235-9-0484. The instrumentation developed to carry out the carefully controlled tests is reported, along with a preliminary analysis of the experimental results. The types of experimental difficulties encountered and some recommendations for improving the quality of the results, with particular concern for increasing their reliability and reproduceability, are also included.

The work represents an extension of earlier research into water migration phenomena in frozen soils, carried out under contract through the Department of Energy, Mines and Resources. The importance of this type of investigation, especially with respect to the long-term frost heave of refrigerated gas pipelines, was set out by Williams and Perfect (1974) in the previous report, contract no. 02SU-KL229-7-1562, and will not be further elaborated here.

As the work progressed a novel approach to the well-known frost cell experiment was developed which appears to have considerable advantage over the conventional form. This involved the construction of a special permeameter which allows, for the first time, direct measurement of thermally actuated water migration in frozen soils. A significant portion of the contract has involved technical work in the construction of this apparatus.

In accordance with the terms of the contract most of the research

was carried out by a graduate student, Mr. E. Perfect, who has just completed his Master's degree on related topics. Indeed, this research constitutes the major portion of Mr. Perfect's thesis. A copy of the thesis, entitled "Temperature-induced water migration in saturated frozen soils", has also been sent to Dr. Judge. Professor Williams has maintained an overall supervising role, as 'Principal Investigator'.

April, 1980 P.J. Williams

II WATER MIGRATION IN FROZEN SOILS: THEORETICAL CONSIDERATIONS

2.1 Unfrozen Water in Frozen Soils

It is well established that significant amounts of unfrozen water coexist with ice in soil at temperatures considerably below $0^{o}C$, the normal freezing point of water (Bouyoucos, 1916; Schofield, 1935; Nersesova and Tsytovich, 1966; Williams, 1967, 1976). Several experimental techniques permit determination of the amount of unfrozen water occurring over the whole range of negative temperatures of practical importance. Results obtained using the various methods are reasonably consistent; they are also in excellent agreement with predictions based on the thermodynamic relationships discussed in the following section. Examples are presented in Figure 2.1 (the curves were determined by J. Wood using the suction-moisture relationship). For most practical purposes the unfrozen water content is determined by temperature and soil type. The amount of unfrozen water at any given temperature below $0^{o}C$ is essentially independent of the amount of ice, and thus of total moisture content. There is a slight dependence on overburden pressure (Williams, 1976).

The presence of unfrozen water in frozen soil is due to capillarity and osmotic effects which reduce its freezing point, and to a variety of adsorption effects associated with soil particle surfaces. Anderson and Hoekstra (1965) have shown by x-ray diffraction that most of the unfrozen water is located immediately adjacent to the particle surfaces. The thickness of these interfacial films has been shown to decrease from

FIGURE 2.1

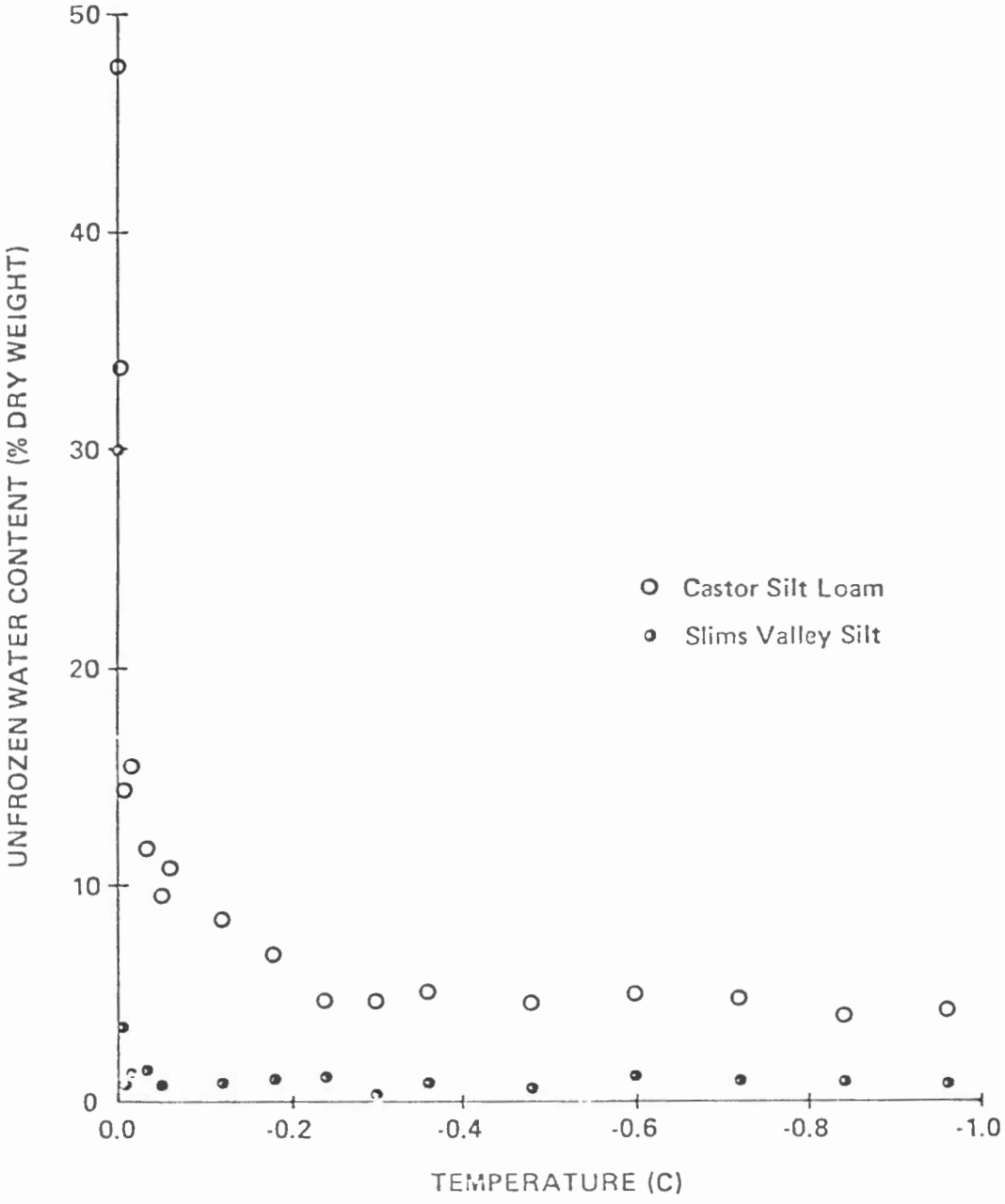

UNFROZEN WATER CONTENTS OF FROZEN SOILS AS A FUNCTION OF TEMPERATURE

5 nm or more at $0^{o}C$ to about 0.9 nm at $-5.0^{o}C$ (Anderson, 1968). A clear and precise relationship exists between film thickness (i.e. unfrozen water content) and the 'suction' associated with the corresponding water content in unfrozen soil (Koopmans and Miller, 1966; Williams, 1967).

2.2 Free Energy and Freezing Point Depression

As the water content of unfrozen soil is progressively reduced, a 'suction' of increasing magnitude develops in the remaining soil water. The dominant cause of this suction is the fall in pore water pressure ascribable to air-water menisci in the soil pores. The phenomenon is described by the well known capillary equation (eg. see Taylor, 1949):

$$H = \frac{2\sigma_{aw}}{r.\rho_{w}.g} \qquad \text{Equation 1}$$

where σ_{aw} = surface tension, air-water interface

ρ_{w} = density of water

g = gravitational acceleration

and H is the height of a column of water supported by a meniscus of radius, r. H may also be equated with the difference in pressure between the air surrounding the soil and the pore water, $\frac{Pa - Pw}{\rho w.g}$; while r can be considered the radius of the soil pores in which the air-water menisci reside (Rose, 1966).

The term 'suction' implies a pressure state. At low water contents this can be misleading since other forces become more important, especially osmotic and surface adsorption effects. For this reason it is preferable to refer to the energy state of the soil water in terms of a more general

thermodynamic function, such as Gibbs free energy. At a constant temperature and pressure the energy state of water, in equilibrium with the soil, can be expressed as the difference in Gibbs free energy of the soil water to that of pure water at atmospheric pressure, that is:

$$\Delta G = G_{sw} - G_w \qquad \text{Equation 2}$$

where ΔG = the relative Gibbs free energy of the soil water (the term 'potential' as defined by the International Society of Soil Science Bulletin of 1965 is equivalent)

G_{sw} = the partial free energy of the soil water

G_w = the partial free energy of pure, bulk water at the same temperature and pressure.

It is not possible to measure absolute free energy, only differences in this quantity. Depending on how 'suction' is defined or measured it may be exactly equivalent to the relative Gibbs free energy (Aitchison et al., 1966).

The energy state of water in an unfrozen, unsaturated soil resembles that of the unfrozen water (at the corresponding moisture content) in a frozen soil. Regardless of whether the remainder of the pore space is filled with air (unfrozen soil) or ice (frozen soil) the free energies of the water are similar; in the case of a frozen soil, Equation 1 is simply modified for an ice-water interface:

$$P_i - P_w = \frac{2\sigma iw}{r} \qquad \text{Equation 3}$$

where σ_{iw} = surface tension, ice-water meniscus.

Thus, the relative Gibbs free energy of the unfrozen water in a freezing

soil changes progressively as the quantity of water is diminished by ice formation. A fundamental equation derived from the Clausius-Clapeyron equation relates Gibbs free energy, ΔG, to freezing point depression (Edlefsen and Anderson, 1943):

$$\Delta G = \frac{(T_o - T)\ell}{T} \qquad \text{Equation 4}$$

where T = temperature

$T_o - T$ = freezing point depression, relative to the freezing point T_o, of pure, bulk water at atmospheric pressure

ℓ = latent heat of fusion.

The equation as defined, only applies in situations where the ice phase is pure and under atmospheric pressure (Williams, 1976). It is the change in free energy associated with a reduction in unfrozen water content, that explains the coexistence of ice and water in soils below $0^{o}C$; the free energies of the ice and unfrozen water are in equilibrium.

Continuous films of unfrozen water extend from the frost-line to points in the frozen soil matrix where temperatures are well below zero. Figure 2.2 shows the relative Gibbs free energy of the unfrozen water as a function of temperature. In many soils capillarity is the dominant effect at temperatures down to about $-1.5^{o}C$ (Williams, 1967). Here Equation 3 is most applicable; values for ΔG essentially corresponding to $P_i - P_w$. Consequently, the potentials generated at such temperatures are normally only a little below the value assigned to pure, bulk water. It is these potentials that are responsible for water movement through the unfrozen zone towards the frostline, the process that causes primary

frost heaving. At colder points within the frozen layer other forces, besides capillarity become important. Here the relative Gibbs free energy of the unfrozen soil water changes entirely in accordance with Equation 4. As indicated by Figure 2.2, the potentials that develop at these points are much lower, in comparison with those originating close to the frost-line. It is these potentials that provide the driving force for water transport through already frozen ground, the process responsible for secondary frost heaving.

2.3 Permeability of Frozen Soils

The existence of continuous liquid films in frozen soil suggests a permeability; in other words, water movement is possible. Transport of unfrozen water can take place in both the liquid and vapour phases, in response to pressure, gravitational, temperature, matric, osmotic and electrical gradients (Anderson and Morgenstern, 1973). In unsaturated frozen soils, vapour transport may play a role provided the pore spaces are not blocked by ice. When the ice content of the frozen soil is high, water movement takes place in the unfrozen, interfacial films. At temperatures close to $0^{\circ}C$, pore ice itself, may become permeable on account of liquid filled crystal boundaries in its structure which act as microscopic channels for water flow (Nye and Frank, 1973; Osterkamp, 1973). Moreover, detailed experimental and theoretical work by Miller (1970) and Miller, Loch and Bresler (1975) suggests that water movement in frozen soils is not restricted to the fluid phases. Under conditions in which a steady

FIGURE 2.2

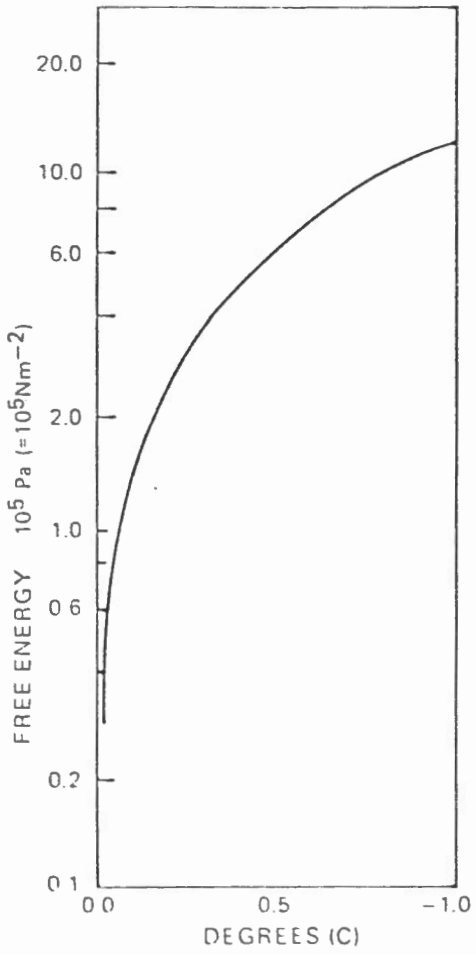

RELATIONSHIP BETWEEN TEMPERATURE AND FREE ENERGY (POTENTIAL) IN FROZEN SOIL.

liquid flux is to be expected, the ice phase may also be conducive to the transport of water by a regelation process. Molecules of unfrozen water move through the frozen, porous medium and freeze on one side of a lens. The latent heat liberated induces thawing on the other side, with a subsequent slow displacement of the ice body towards the melting face. It follows that the presence of ice lenses may not be much of a barrier to flow, even through no direct path exists (Burt and Williams, 1976).

Several procedures have been suggested for the measurement of the apparent hydraulic conductivity of frozen soils. Harlan (1973) has advocated the use of hydraulic conductivity values obtained for unsaturated, unfrozen soils, on the assumption that the permeability at a given liquid water content is the same in the frozen as in the partially saturated state. Unfortunately, this analogy breaks down somewhat, as soon as ice lensing occurs in the frozen soil. The amount of unfrozen water present at any given temperature is independent of the total moisture content, but an increase in the latter gives additional ice, which may significantly alter the conditions of flow.

Alternatively, Burt and Williams (1976) developed a permeameter for the direct measurement of water movement in frozen soils. The apparatus is similar to that used to measure the hydraulic conductivity of unfrozen, saturated soils, but with various modifications to accommodate the presence of a frozen sample (Figure 2.3). The experiment is carried out under isothermal conditions, and involves the passage of water from one reservoir

FIGURE 2.3

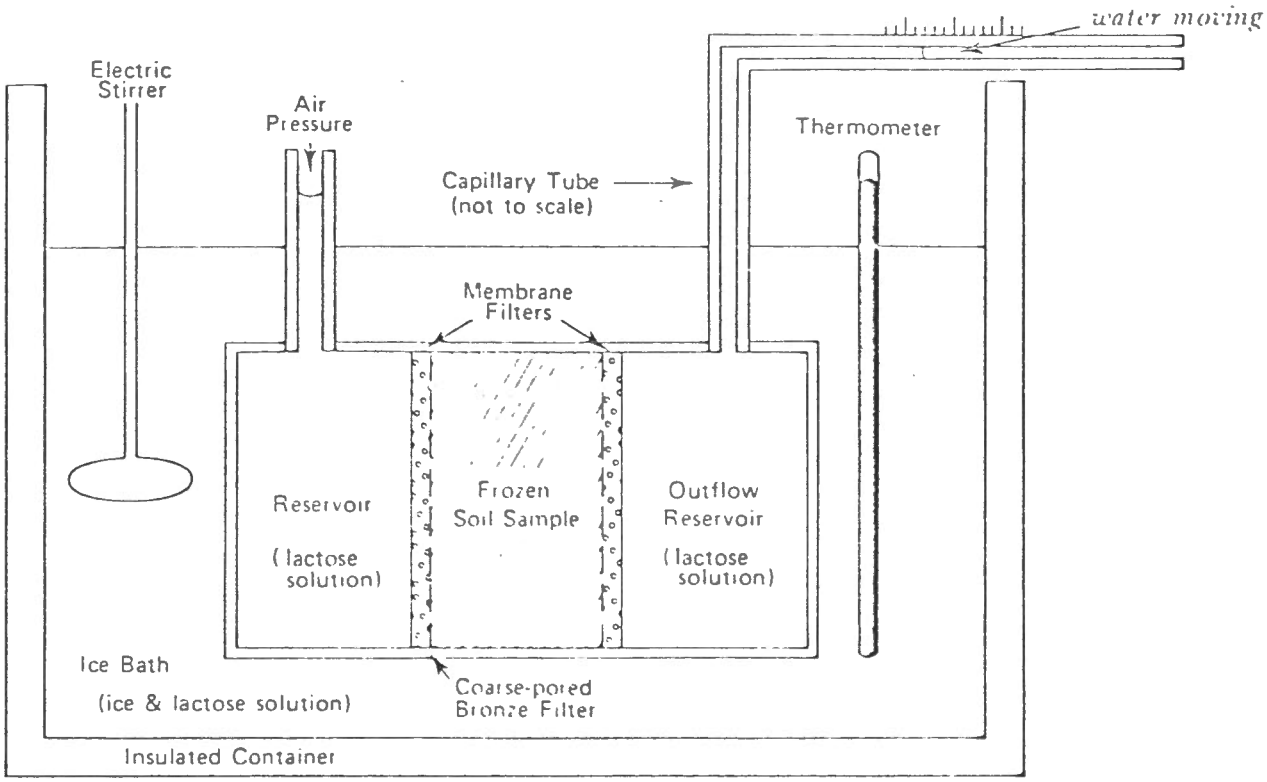
water moving
Electric Stirrer
Air Pressure
Capillary Tube (not to scale)
Thermometer
Membrane Filters
Reservoir (lactose solution)
Frozen Soil Sample
Outflow Reservoir (lactose solution)
Ice Bath (ice & lactose solution)
Coarse-pored Bronze Filter
Insulated Container

into the frozen sample and out into a second reservoir. The water in the reservoirs remains unfrozen because it contains dissolved lactose. The potential gradient is supplied by application of hydrostatic pressure to one reservoir.

The interpretation of hydraulic conductivity coefficients is made difficult by the complex thermodynamic situation in frozen soils. There is little doubt however, that water, in one phase or another, is able to move through frozen soil in significant quantities, particularly at temperatures within a few tenths of $0^{o}C$. The latter is to be expected because of the relatively large amounts of unfrozen water at these temperatures. Figure 2.4 shows the apparent hydraulic conductivity-temperature relationships for Castor silt loam and Slims Valley silt. The curves were determined by the present authors using a modified version of the Burt and Williams permeameter (Williams and Perfect, 1979). The results are compatible with permeability values for frozen soils measured earlier (Burt, 1974). It can be seen that conductivities generally increase as the temperature rises towards $0^{o}C$; commonly observed values being in the range 10^{-8} to 10^{-12} m. sec^{-1}.

2.4 Temperature Induced Water Migration in Frozen Soils

A temperature gradient in frozen soil implies a gradient of potential according to the relationship between Equation 4 and Figure 2.2. Thus, a flux of water is to be expected in the direction of decreasing temperature. It should be noted, that in a system with a temperature gradient, thermodynamic equilibrium in a precise sense does not exist; thus Equation 4

FIGURE 2.4

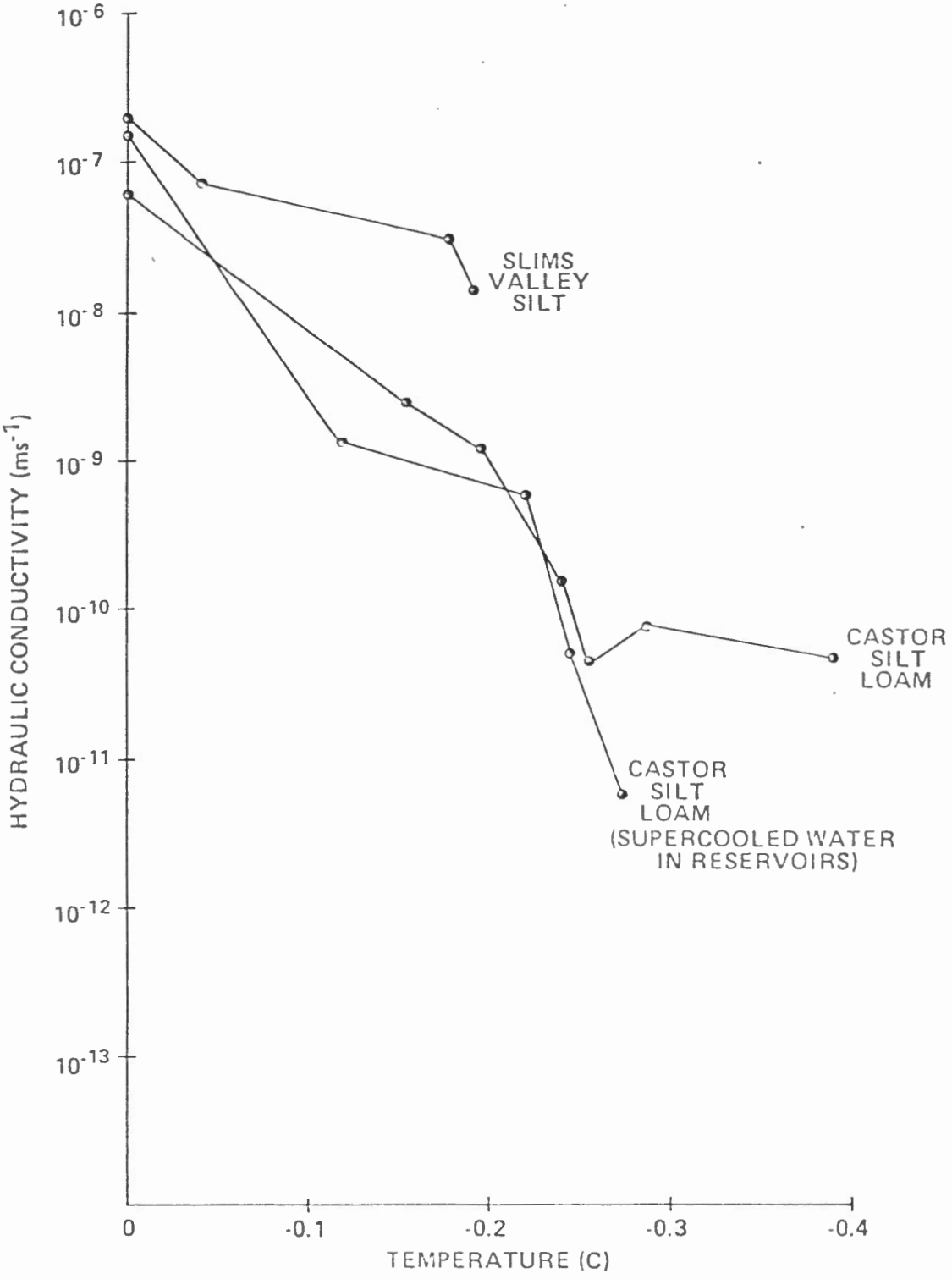

HYDRAULIC CONDUCTIVITIES OF FROZEN SOILS AS A FUNCTION OF TEMPERATURE. (EXPERIMENTAL DETERMINATIONS).

is not strictly applicable. The amount of moisture migration will also depend upon the apparent hydraulic conductivity of the soil in the frozen state.

III EXPERIMENTAL PROCEDURE

3.1 Apparatus Design

This study is concerned with water migration in saturated frozen soils under applied temperature gradients. An experiment has been designed which allows, for the first time, direct measurement of such movements. The basic apparatus consists of a frozen soil sample placed between two bodies of water. On application of a temperature gradient across the system, the frozen soil can be expected to act in general, as a kind of pump, inducing water migration in the direction of decreasing temperature. This is in accordance with the relationship between temperature and free energy (Equation 4) illustrated in Figure 2.2. Several important requirements must be met, however, in the construction of an experimental apparatus to investigate this phenomenon:

1. The water in the reservoirs must be at the same temperature as the ends of the frozen soil sample. The juxtaposition of ice and pure, bulk water will however, cause freezing of the latter at any temperature below $0^{o}C$. Therefore, the potentials of the water in the reservoirs and the unfrozen soil water must be equalized before a temperature gradient is established across the system.

2. Both ends of the sample must be held at constant temperatures below zero. Because heat flow through the frozen sample may be variable, it is desirable to have the end plates controlled by a device which is able to maintain the required sub-zero temperature with rapid adjustment to fluctuations in cooling load.
3. Heat flow must be uniaxial. If this is not the case, then the temperature and moisture distribution will not be uniform (in cross-section) at any given distance along the sample. It is necessary therefore, to minimize any radial heat exchange between the sample and its surroundings.

The design of the complete experimental apparatus is shown in Figure 3.1 (a scale drawing of the sample cell and end plates is given in Appendix I). In construction it is similar to that used by Burt and Williams (1976) to measure the hydraulic conductivity of frozen soil samples under isothermal conditions. The essential difference is that the hydraulic gradient is induced by a thermal gradient rather than by a pressure differential.

The soil sample is contained in a plexiglass cylinder, 3.175 cm long, with a wall thickness of 1.90 cm and an inside diameter of 5.40 cm. The cylinder and reservoirs are sandwiched between two Aluminum end plates containing Peltier modules. These cooling devices are controlled by a thermo-electric cooling control system which can maintain temperatures constant to within $\pm$ 0.02^{o}C under steady state

The jacket of fibreglass insulation that the cell is wrapped in is not shown.

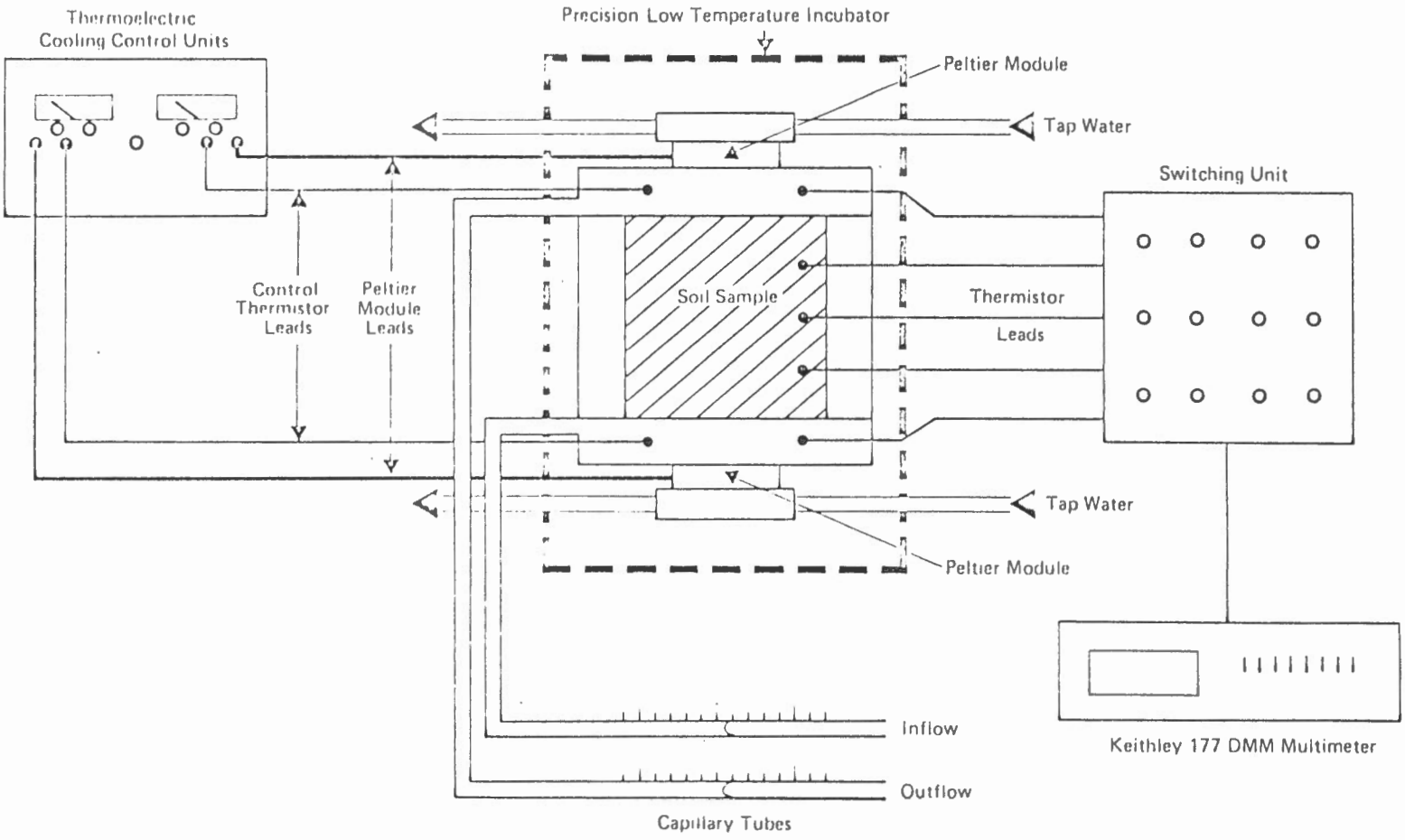

SCHEMATIC DIAGRAM OF THE COMPLETE EXPERIMENTAL APPARATUS
(SEE APPENDIX I FOR SCALE DRAWING OF THE CELL AND END PLATES).

FIGURE 3.1

conditions (Williams, 1968). The soil sample is held firmly in place by two porous brass plates which are in thermal contact with the thermo-electric cooling plates.

3.2 Preparation of Soil Samples

All samples are prepared as slurries. This is normally done by saturating the soil under vacuum with deaired, deionized water. The sample is then frozen into the plexiglass cylinder. The method of freezing governs the type and pattern of ice lenses. To minimize moisture redistribution during freezing (the process responsible for ice lensing) the sample is frozen rapidly from all directions in a refrigerator, and then warmed to a temperature of approximately $-0.5^{\circ}C$. Before assembly the ends of the frozen sample are scraped with a metal blade to give a plane surface, flush with the plexiglass cylinder. Two soils were used in the experiments, Castor Silt loam and Slims Valley Silt. Grain size distributions for these soils are shown in Figure 3.2. Slims Valley Silt was used in experiments 1, 2 and 6, and Castor Silt loam in experiments 3, 4 and 5.

3.3 Prevention of Freezing in the Reservoirs

Unfrozen water in frozen soil possesses a suction or potential relative to free, pure water at the same temperature due to capillarity, dissolved salts and a variety of adsorption effects (see Section 2.2). Consequently, if pure water was placed in the reservoirs, even if freezing did not occur, there would be a tendency for it to be pulled into the

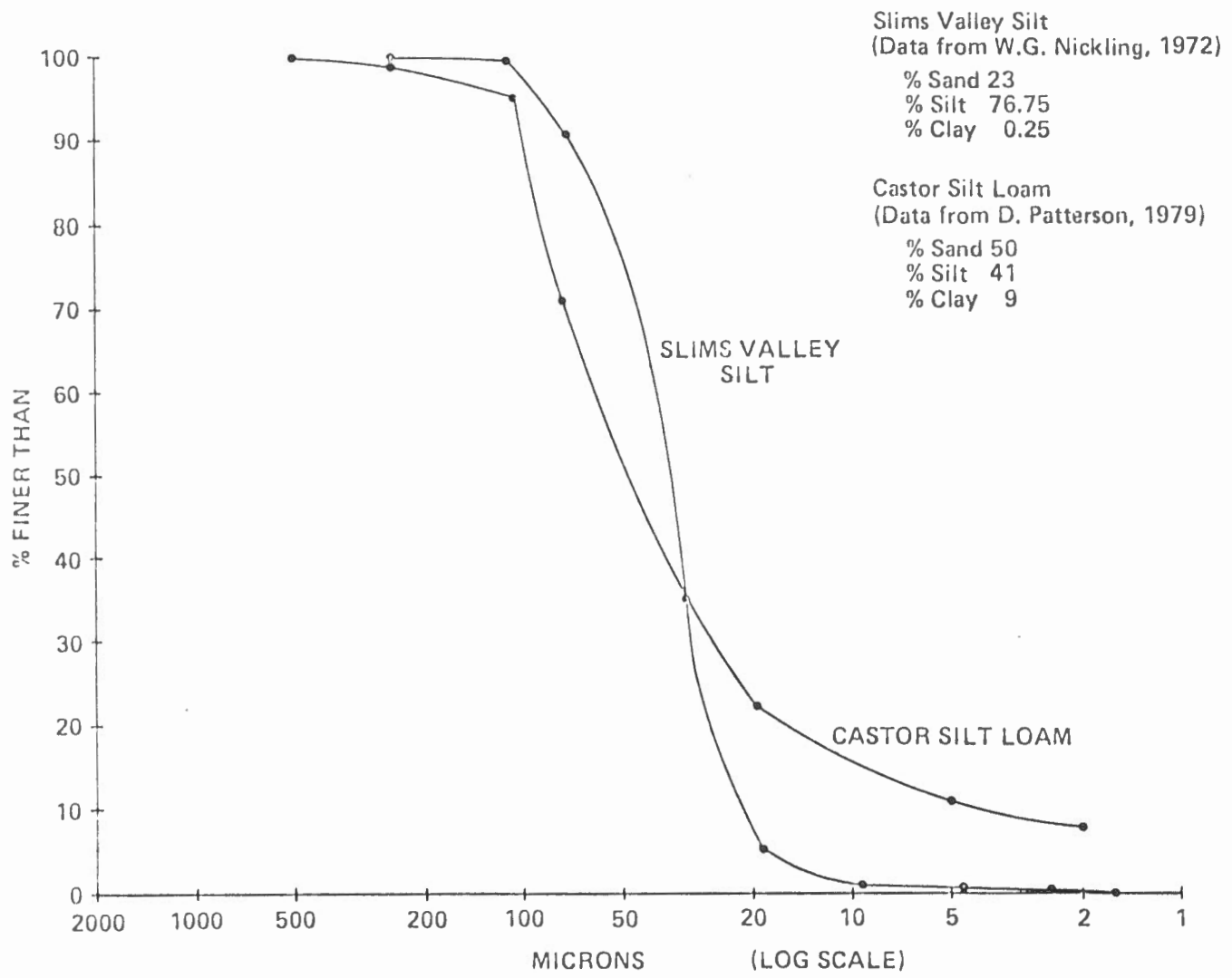

GRAIN SIZE ANALYSIS FOR SOILS USED IN THE EXPERIMENTS.

FIGURE 3.2

frozen sample. The potentials of the water in the reservoirs, and the unfrozen soil water can be equalized by creating an osmotic potential in the reservoirs. With respect to a pool of pure water at atmospheric pressure, unfrozen water in frozen soil and an aqueous solution of lactose are both subject to a decrease in Gibbs free energy. Since the potential of the unfrozen water is fixed for any negative temperature, the concentration of lactose can be adjusted so as to produce a corresponding decrease in free energy of the water in the reservoirs. The concentration required to produce the correct osmotic potential is easy to obtain for any given temperature (see Appendix II).

On assembly the reservoirs are normally filled with lactose solution, as with the Burt and Williams permeameter. Since the present experiment is non-isothermal, the concentrations should ideally be different in the two reservoirs. In the tests reported here however, a concentration giving a freezing point depression equivalent to the 'cold' end temperature was used in both reservoirs. It follows that the potentials of the unfrozen soil water and the lactose solution at the 'cold' end are in equilibrium. This procedure however, coupled with the presence of dialysis membranes (see next paragraph) results in a local osmotic potential gradient at the 'warm' end of the sample, which could induce flow in the opposite direction to the thermally actuated hydraulic gradient. This effect is discussed in detail in Section 5.1.

The presence of lactose in the reservoirs creates the possibility of lactose molecules moving into the sample either by molecular diffusion,

or through transport in water moving from the inflow reservoir. A dialysis membrane is therefore fitted on each end of the frozen sample to impede entry of the lactose molecules into the unfrozen soil water. Because of their small molecular size however, the lactose molecules are still able, to some extent, to pass through this semi-permeable membrane. The passage of lactose into the sample raises the potential of the unfrozen water, with the result that some pores become ice free (this effect is discussed further in Section 5.2).

3.4 The Use of Supercooled Water

Two experiments (Experiments 5 and 6) were run with the present apparatus in which pure water, previously deionized and deaired was used in the end reservoirs. The dialysis membranes served as effective phase barriers separating pore ice from the supercooled water in the reservoirs. The porous brass plates were replaced by aluminum discs, with machined surfaces and smooth pores. The brass plates have jagged surfaces which could puncture the membranes and thereby permit ice propagation into the reservoirs. The irregularities might also serve as nucleation sites for ice growth. The results from these experiments proved to be somewhat unexpected, since flow appeared to take place in the opposite direction to the hydraulic gradient implied by the temperature profile. See Section 4.5 for a detailed discussion on this topic.

3.5 Establishment of a Linear Temperature Gradient

A gradient of potential is induced by imposing a linear temperature

gradient across the frozen sample. This is done by maintaining the two thermo-electric cooling plates at different sub-zero temperatures. The time required to establish an approximately linear temperature gradient was about 12 hours in all experiments. An example is shown in Figure 3.3 (the constant end temperatures represent the temperatures of the thermo-electric cooling plates). The gradient is increased in a stepwise fashion, with measurements delayed for at least 6 hours, but often over night to allow for re-equilibration. Concurrently the reservoirs are flushed with a fresh supply of lactose solution, the concentration of which corresponds to the new 'cold' end temperature. It should be noted that although the temperature profile approaches a steady state situation on a macroscopic scale, there will be continual microscopic perturbations associated with coupled heat and moisture transport.

To minimize radial heat exchange between the frozen sample and air at room temperature, the apparatus is wrapped in a jacket of fibreglass insulation, approximately 5 cm thick. The entire assembly is then placed in a 'Precision' low temperature incubator which maintains a uniform air temperature of approximately $0^{\circ}C$. The fact that a nearly linear temperature gradient is achieved suggests that radial heat exchange is relatively small compared with axial heat flow. Continuous monitoring of the temperature profile is provided by five calibrated thermistors (estimated limit of accuracy $\pm 0.01^{\circ}C$) located along the sample holder and in the end plates. The tips of the thermistors extend about 0.25 cm into the frozen soil.

FIGURE 3.3

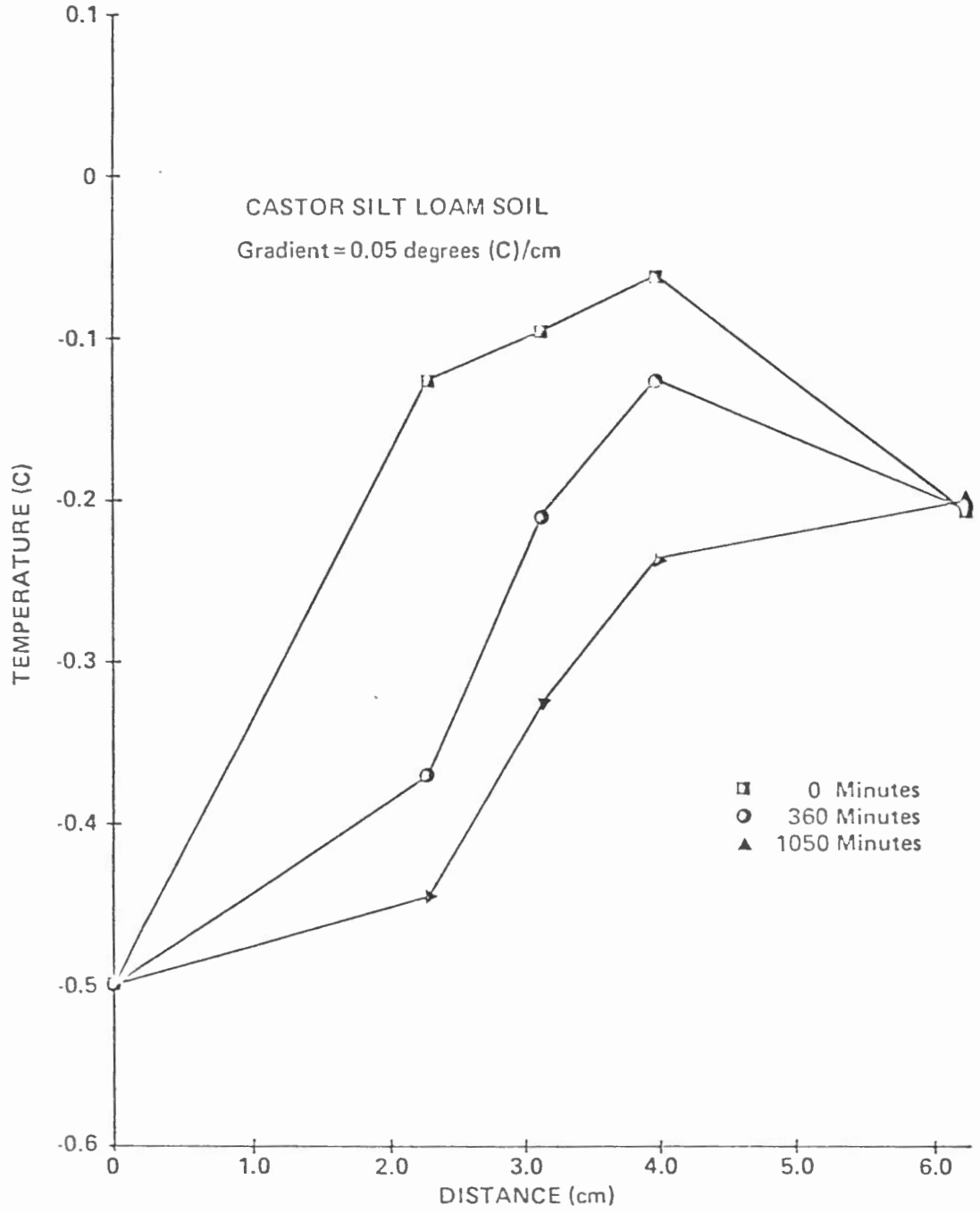

APPROACH TO LINEARITY IN THE TEMPERATURE PROFILE. (EXPERIMENT NO. 4A)

3.6 Measurement of Flow

Once a stable, linear temperature gradient is established across the system, water appears to pass from the 'warm' reservoir into the frozen sample, and out into the second, colder reservoir. Inflow and outflow are measured by timing the movement of menisci along capillary tubes. Readings are taken every thirty minutes for a period of six hours. This procedure may be repeated over a number of days. The observed velocities are converted into a volume using the radii of the capillary tubes (determined to be 0.025 cm).

3.7 Calculation of Hydraulic Conductivity Coefficients

On application of a temperature gradient across the system the frozen soil acts in general as a kind of pump, inducing water migration in the direction of decreasing temperature. Since the temperature profile appears to be linear, at least on a macroscopic scale, the implied gradient of potential must also be linear in nature. This means that we can use the generalized form of Darcy's Law, in conjunction with the implied potential gradient, and the volume of outflow, to calculate an approximate, mean hydraulic conductivity coefficient for the frozen sample. Thus, Equation 5 can be re-written in the form:

$$q = -\bar{K}.A.\frac{d\Psi}{dx} \simeq \frac{-\bar{K}.\Delta h.A}{L} \qquad \text{Equation 6}$$

where $\bar{K}$ = mean hydraulic conductivity of the frozen sample

Δh = potential expressed in cms of water head

A = sample cross-sectional area

L = path length of flow

It follows that:

$$\bar{K} = \frac{q.L}{\Delta h.A} \qquad \text{Equation 7}$$

The flux, q, is given by the equation:

$$q = \pi r^2 \frac{d}{t} \qquad \text{Equation 8}$$

where r = radius of the capillary tube

d = distance travelled by the meniscus in time, t.

Since L, A and r^2 are constants in the design of the apparatus ($L = 3.175$ cm; $A = 22.88$ cm^2; and $r^2 = 6.25 \times 10^{-4}$ cm^2):

$$\bar{K} \simeq \frac{d.c}{t.\Delta h} \qquad \text{Equation 9}$$

where c = the product of the constants, which equals 2.725×10^{-4} for the dimensions of the present apparatus. Thus, an estimate of the mean hydraulic conductivity coefficient is given by:

$$\bar{K} = \frac{2.725 \times 10^{-4}.d}{t.\Delta h} \qquad \text{Equation 10}$$

It follows that calculation of $\bar{K}$ involves measurement of d, t and Δh. The values of d and t can be obtained directly, while Δh can be deduced from the temperature profile, as in the following example:

In an experiment with a Castor Silt loam soil (see Appendix III, Expt. 4B), the cooling plates at either end of the sample were maintained at temperatures of -0.2 and -0.5°C respectively, giving a temperature gradient of 0.048°C/cm. The mean temperature was -0.35°C. According to Equation 4 (see Section 2.2): The potential generated at -0.2°C $\simeq 2.469 \times 10^5$ Nm^{-2} and the potential generated at -0.5°C $\simeq 6.173 \times 10^5$ Nm^{-2}

The difference between these two values gives the potential, generated over the length of the sample, which equals 3.704×10^{5} Nm^{-2} (equivalent to 3,704 cm of water head).

Given that the capillary meniscus moved 0.25 cm in 1800 seconds, the mean hydraulic conductivity coefficient is:

$$\bar{K} = \frac{2.725 \times 10^{-4} \; .0.25}{1800.3704} \quad cm\ s^{-1} \qquad \text{Equation 11}$$

$$\therefore \bar{K} = 1.02 \times 10^{-13}\ m\ s^{-1}$$

It must be remembered that hydraulic conductivity is a function of the temperature profile, and that $\bar{K}$ represents an "average" value, over the length of the frozen sample. Moreover, the experiment should not be viewed strictly as a permeability test. In conventional hydraulic conductivity tests the discharge is normally directly proportional to the hydraulic gradient applied; this follows from Equation 6. In the experiments described here however, the applied temperature gradient gives rise to an internal driving force (i.e. the pump analogy). Since a change in the potential gradient necessarily involves an alteration of the temperature profile, there must also be a corresponding change in unfrozen water contents. This, in turn, implies a change in the sample's apparent hydraulic conductivity. Thus, a direct linear relationship between discharge (meniscus velocity) and potential gradient is not to be expected.

IV RESULTS AND DISCUSSION

All relevant data collected during the experiments are presented in Appendix III. The discussion can logically be divided into two separate

themes. Firstly, it is convenient to consider the observations in terms of the current theoretical understanding of frozen soils, as outlined earlier. In this chapter a tentative, phenomenological evaluation of the results will be presented, attention being paid to the variation of flow rates with respect to thermal gradients, mean temperatures and soil properties. However, certain properties associated with the experiment itself, produce effects which may modify the observations. This represents the second theme of the discussion, presented in the following chapter.

4.1 Relationship Between Flow Rate and Temperature Gradient

For most tests stable and essentially linear temperature gradients were established across the system, as this served to simplify interpretation of the results. During the approach to linearity in the temperature profile, a steady flux of water was normally observed entering the reservoirs at both ends of the frozen sample. An example of this phenomenon is illustrated in Figure 4.1. An examination of Figure 3.3 indicates that initially both thermo-electric cooling plates were colder than the interior of the frozen sample. Presumably the sample warms somewhat during assembly of the apparatus. Consequently water tends to leave the frozen soil from both ends, in accordance with the relationship between temperature and free energy (Equation 4). This implies a net loss of water from the soil, until an approximately linear temperature gradient is achieved across the system.

One experiment was run using a Slims Valley Silt soil (experiment No. 2A)

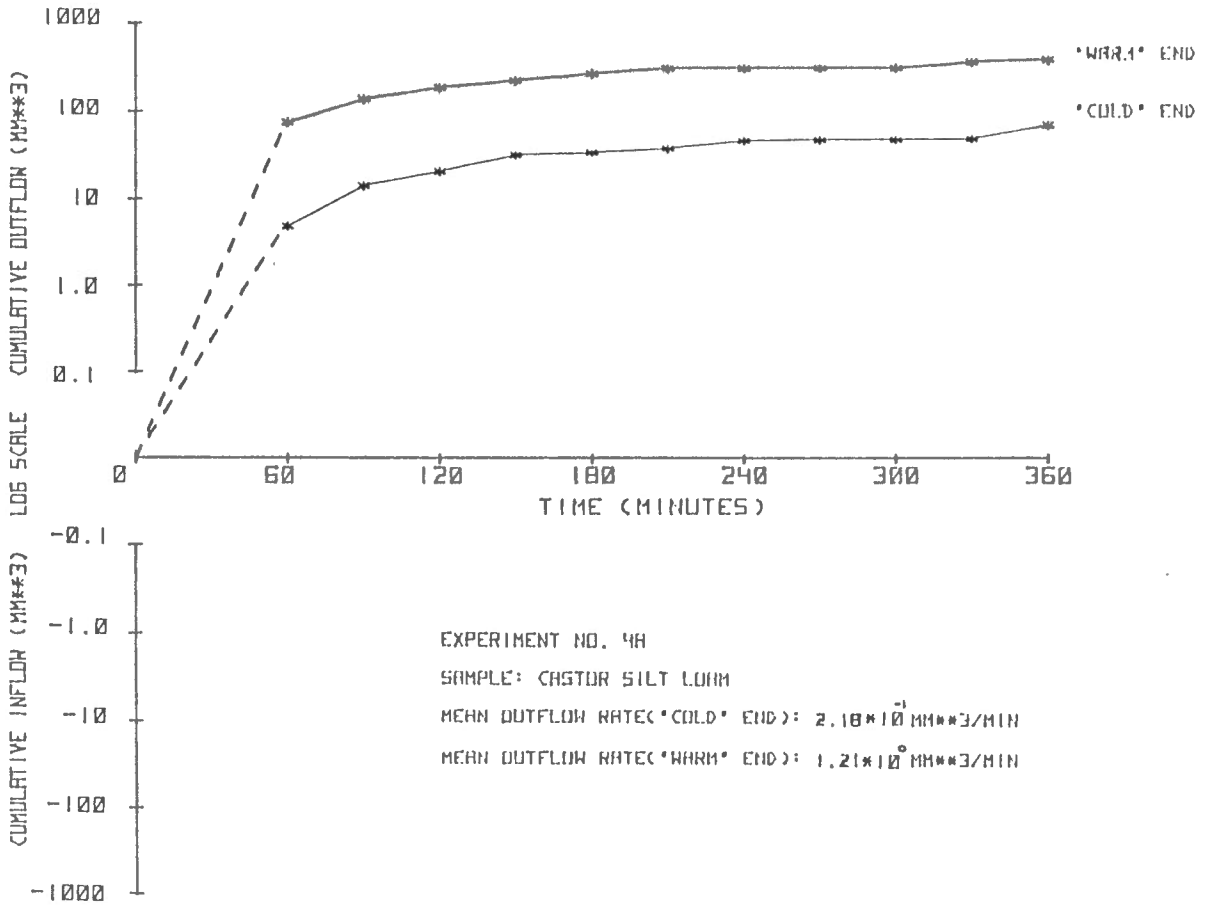

FIGURE 4.1 CUMULATIVE OUTFLOW DURING APPROACH TO LINEARITY IN THE TEMPERATURE PROFILE

in which there was no temperature gradient across the sample. Both thermo-electric cooling plates were maintained at a constant temperature of $-0.325^{\circ}C$, while the reservoirs contained the same concentration of lactose solution, adjusted to give the appropriate freezing point depression. Once stable temperatures were achieved, cumulative inflow and outflow were observed to be negligible (see Appendix III). Since no driving potential was generated, and the potentials of the lactose solution in the reservoirs, and the unfrozen soil water were in equilibrium, there was no tendency for water to be pulled into or out of the frozen sample.

When a stable, linear temperature gradient is established across the system, a fairly steady flux of water appears to take place in the direction of decreasing temperature. This is consistent with the theory outlined in Section 2.4. Water normally passes from the 'warm' reservoir into the frozen soil, and there is an outflow into the second, colder reservoir. The rate of flow will be governed by the magnitude of the temperature gradient (i.e. the potential for water movement), the mean temperature of the frozen sample (i.e. the apparent hydraulic conductivity), and the soil type. Generally, mean rates of inflow were less than the outflow by approximately an order of magnitude, which implies a net loss of water from the frozen soil sample. In one respect a net gain might be expected since permeability decreases non-linearly with temperature (see Figure 2.4), while the potential decreases linearly. However, certain properties associated with the test procedure itself, produce effects

which could account for this observed disparity between rates of inflow and outflow. These are discussed in detail in the following chapter.

For similar soils the flux should be a play-off between two factors: the gradient of potential and the permeability-temperature relationship. In the tests reported here, samples at the same mean temperature, showed a marked increase in flow rates with increasing temperature (potential) gradient. For example, Figures 4.2 and 4.3 show cumulative inflow-outflow over time for two samples (Castor Silt loam and Slims Valley silt) at approximately the same mean temperature ($-0.25^{o}C$). The temperature gradients were 0.016 and $0.0896^{o}C/cm$ respectively, giving potential gradients of 1.235×10^{5} N m^{-2} and 6.420×10^{5} N m^{-2}. It can be seen that cumulative outflow is well over an order of magnitude greater with the larger temperature (potential) gradient.

It should be remembered that the tests were carried out at relatively warm mean temperatures (i.e. in the range 0 to $-0.5^{o}C$), where the variation of apparent hydraulic conductivity with temperature is considerable. At lower mean temperatures the permeability-temperature relationship levels off; here one would expect the temperature (potential) gradient to become the predominant factor. It is unlikely however, that an increase in the gradient would significantly increase fluxes, due to the limiting effect of the extremely low conductivities below about $-0.5^{o}C$.

With a step-wise increase in the temperature gradient a temporary surge in the amount of outflow was observed. For example, Figure 4.4 shows the effect on cumulative outflow of increasing the temperature

FIGURE 4.2 CUMULATIVE INFLOW-OUTFLOW INDUCED BY A
RELATIVELY SMALL TEMPERATURE GRADIENT

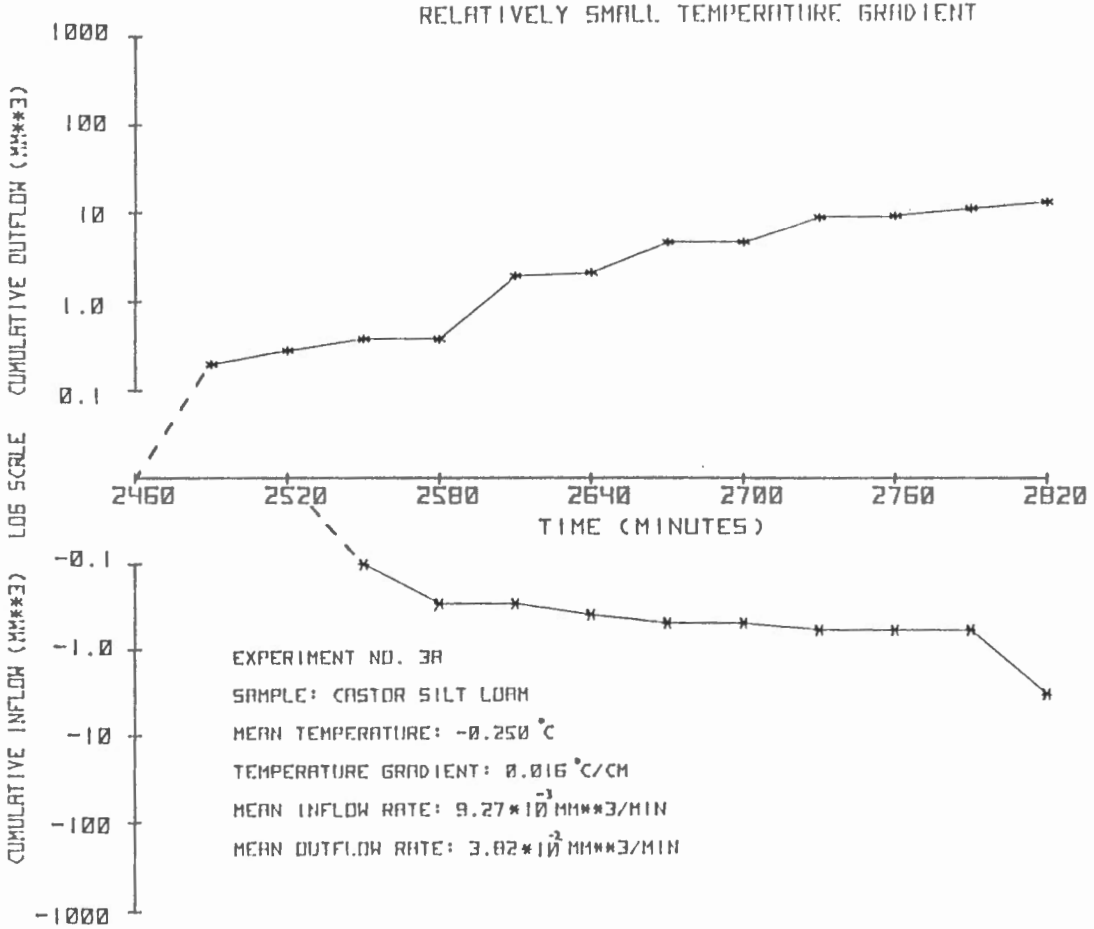

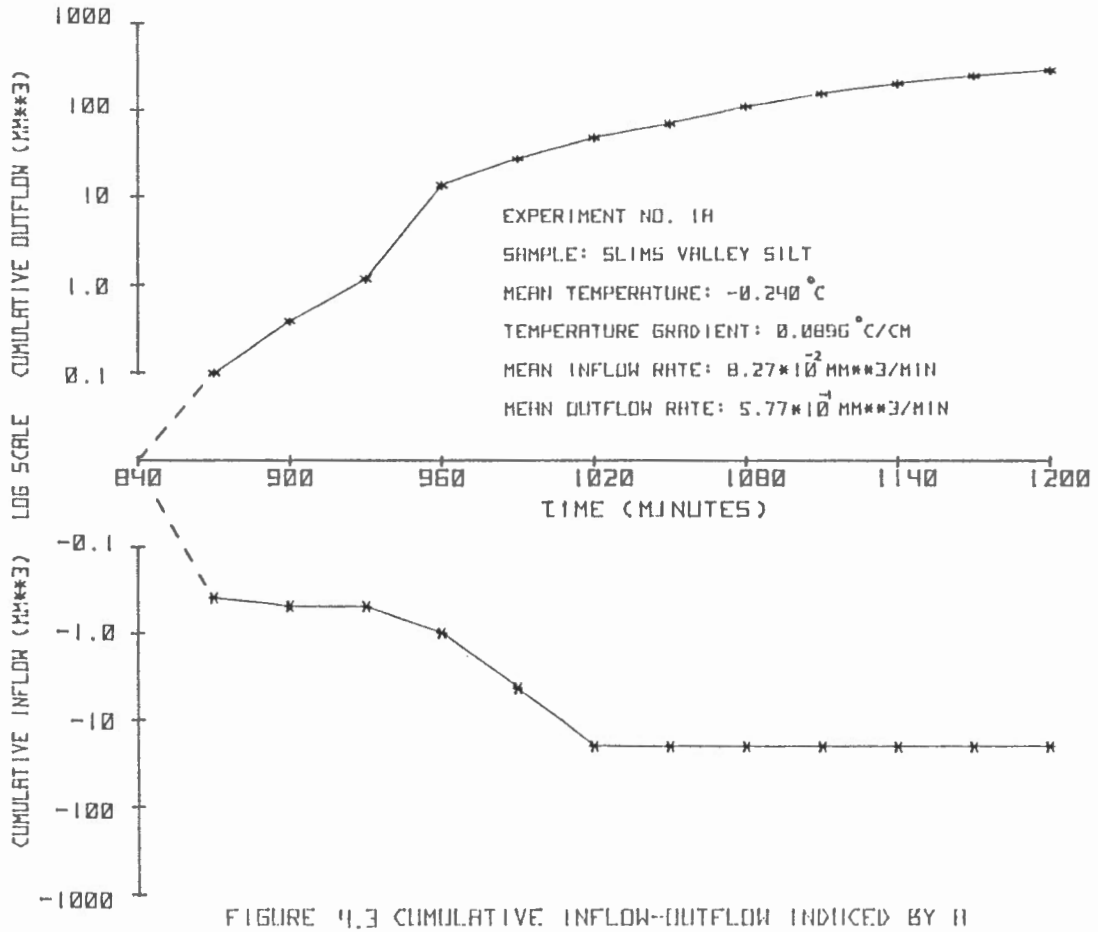

FIGURE 4.3 CUMULATIVE INFLOW-OUTFLOW INDUCED BY A RELATIVELY LARGE TEMPERATURE GRADIENT

FIGURE 4.4 CUMULATIVE OUTFLOW DURING A STEP-WISE INCREASE IN THE TEMPERATURE GRADIENT

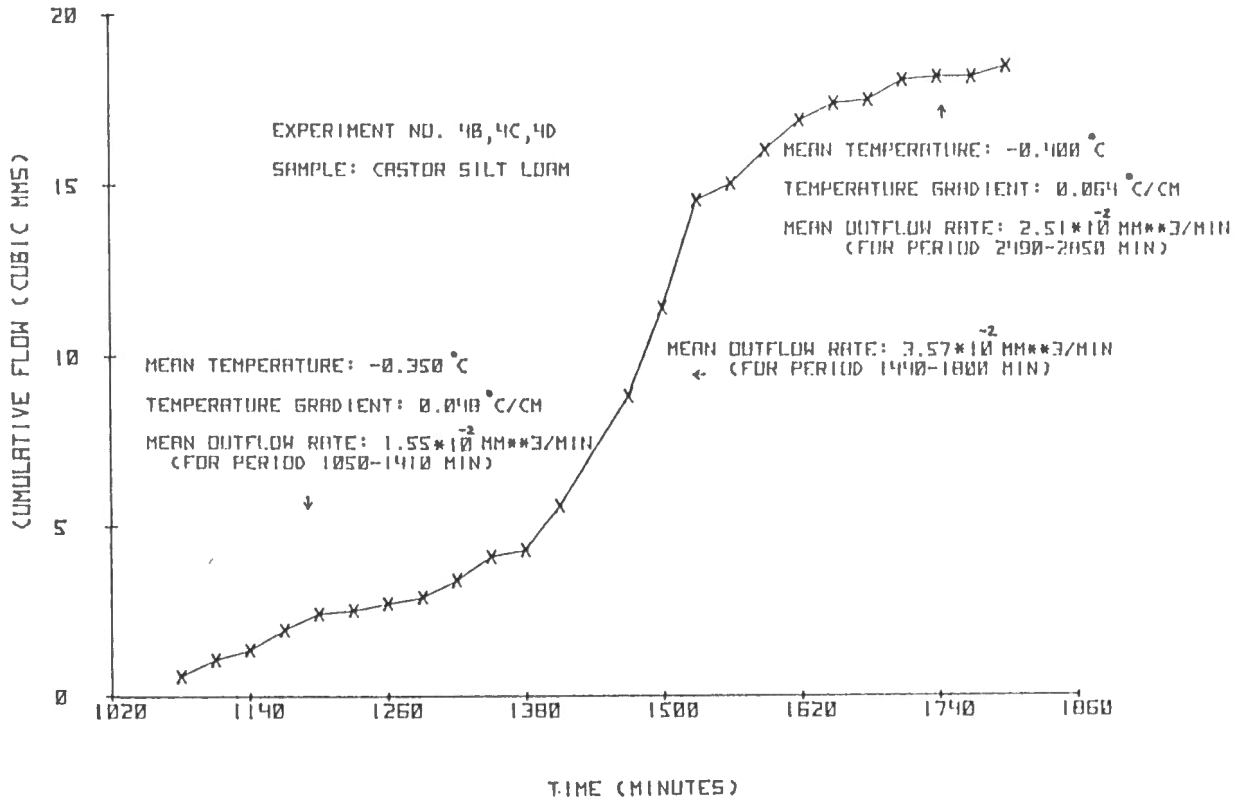

gradient from 0.0480°C/cm to 0.0640°C/cm. The sample used was a Castor Silt loam soil. Initially, with the stable temperature profile, it can be seen that outflow rates were fairly steady (mean of 1.55 X 10^{-2} mm^3/min). Following the step change in the temperature gradient there is a distinct increase in the outflow rate (mean of 3.57 X 10^{-2} mm^3/min). This effect is only temporary however, and flow rates soon level off, to reach a new steady state (mean of 2.51 X 10^{-2} mm^3/min) as the temperature profile re-establishes its linearity. It should be noted that flow rates achieved with the new temperature gradient are slightly greater than those measured earlier. The surge was not observed with rates of inflow, although this is not surprising since the step changes were always effected by lowering the temperature of the 'cold' end plate.

4.2 Temperature Dependence of Flow Rates

The same temperature gradient applied across similar soils should induce different rates of flow depending on the mean temperature of the frozen samples. This follows directly from the reduction in hydraulic conductivity with decreasing temperature (see Figure 2.4). In other words, a specific gradient of temperature (potential) can be expected to yield a greater flux at temperatures close to 0°C (i.e. relatively high hydraulic conductivities) than at colder mean temperatures. This is illustrated in Figures 4.5 and 4.6, which show cumulative inflow-outflow over time for similar samples (Slims Valley silt and Castor Silt loam), with mean temperatures of -0.16° and -0.35°C respectively. The temperature

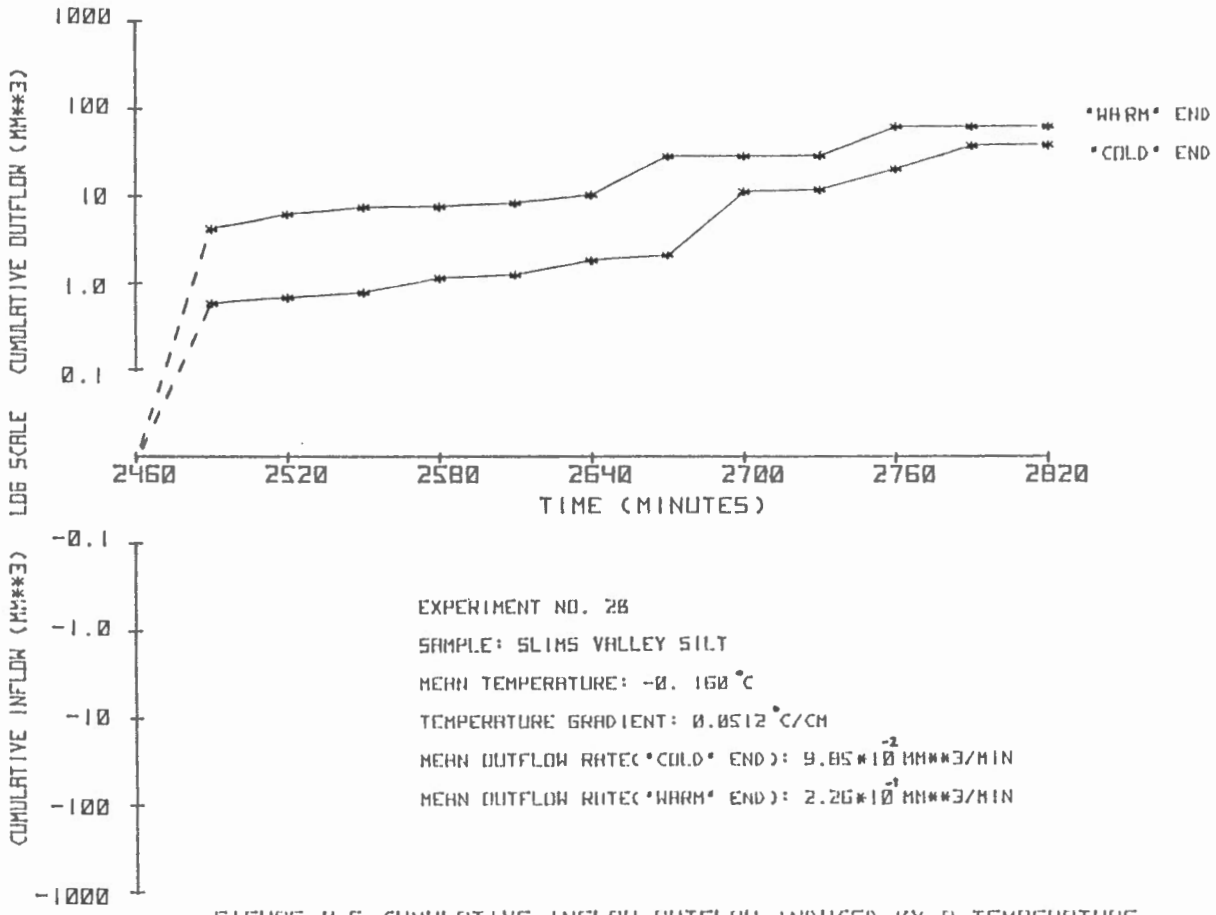

FIGURE 4.5 CUMULATIVE INFLOW--OUTFLOW INDUCED BY A TEMPERATURE GRADIENT AT A RELATIVELY WARM MEAN TEMPERATURE

FIGURE 4.6 CUMULATIVE INFLOW-OUTFLOW INDUCED BY A TEMPERATURE GRADIENT AT A RELATIVELY COLD MEAN TEMPERATURE

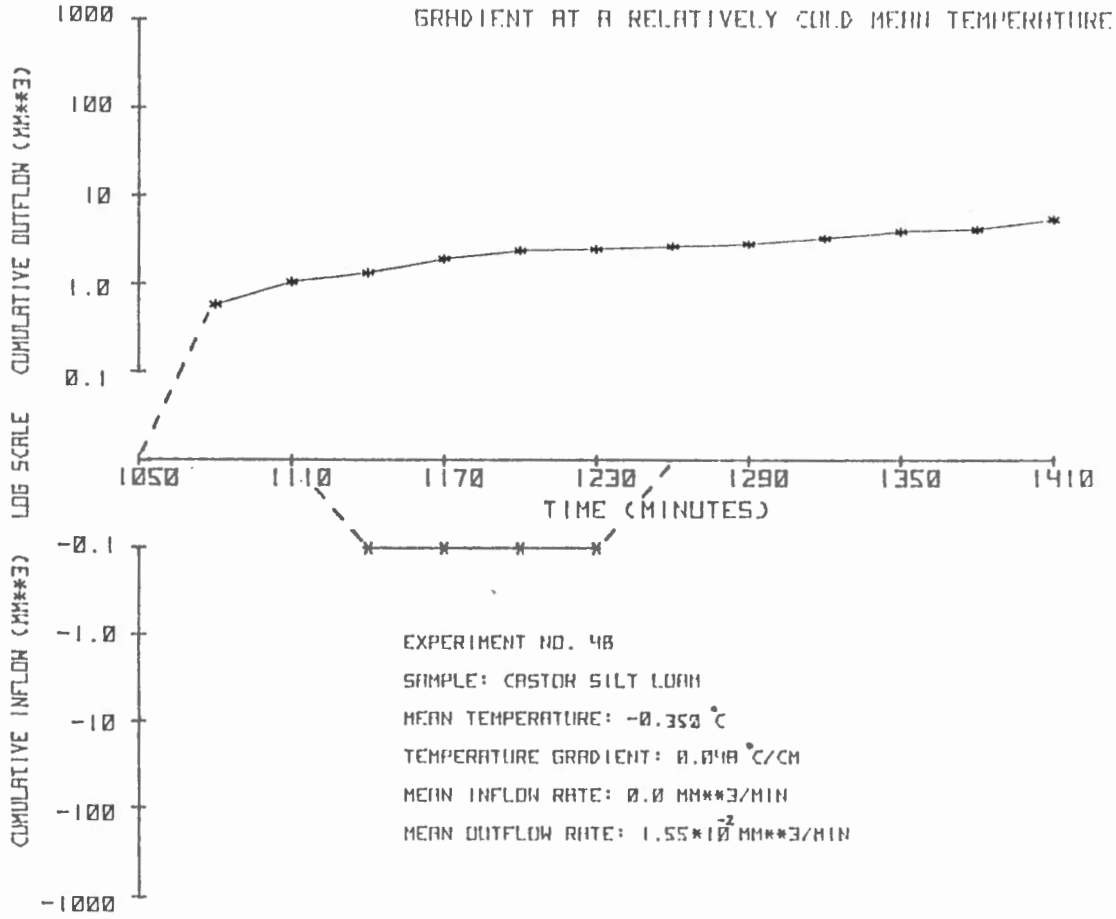

gradient in both cases was approximately 0.05°C/cm. This gradient produced a mean outflow rate of 9.846 X 10^{-2} mm^3/min. One would expect this drop-off in flow rates to continue with decreasing temperature, so that permeability becomes the limiting factor, regardless of the size of the temperature induced gradient of potential. Examination of Figure 4.5 reveals that outflow took place from both ends of the sample in experiment No. 2B. This may be due to the existence of a reverse osmotic potential gradient across the membrane at the 'warm' end of the sample. This gradient could be sufficient to locally counteract the temperature induced gradient of potential, with the result that water moves out of the frozen soil into the 'warm' reservoir. This effect is dealt with in detail in Section 5.1.

4.3 Variation of Flow Rates with Soil Type

One can expect some variation in flow rates as a result of soil type. The unfrozen, water content and apparent hydraulic conductivity of a frozen soil appear to be related through pore size distribution, void ratio and surface area. These factors are themselves related to the grain size characteristics of the soil. Consequently, a temperature gradient applied across two different soils, at approximately the same mean temperature may produce different volumes of discharge, depending on the grain size distribution of the soils.

Discussion of the influence of grain-size on unfrozen water content and apparent hydraulic conductivity sheds light on the relationship between

soil type and flow rate. However, an explicit comparison is impossible here, since the two soils used in the experiments possessed rather similar grain-size distributions. The reader is referred to Burt (1974) p. 39-48 for a more detailed treatment, albeit with respect to the isothermal situation, of the relationship between particle size and permeability. Further research is needed with the present apparatus to clarify the influence of soil type on thermally actuated water movements. This must obviously include the testing of a large number of different soils, for which unfrozen water content-temperature relationships, and grain-size distributions are known.

4.4 Temperature and Apparent Hydraulic Conductivity

The hydraulic conductivity coefficients were calculated from measured volumes of outflow, in conjunction with derived gradients of potential, according to the procedure described in Section 3.7. Calculated values for $\bar{K}$ are presented in Table 4.1, along with the range of temperatures for which the results are valid. Theoretically, $\bar{K}$ represents the apparent hydraulic conductivity-temperature relationship averaged over the length of the frozen sample. In practice however, $\bar{K}$ will be closer to the limiting, or lowest permeability at the 'cold' end of the sample. Assuming that this is the case, then it is most useful to investigate variations in $\bar{K}$ with respect to 'cold' end temperatures.

For tests run on the same sample, it can be seen that conductivities generally decrease with decreasing 'cold' end temperature, although the data do not compare well between samples. It should be remembered that

Table 4.1 Hydraulic Conductivity Coefficients*

Experiment No.		'Cold' end temperature (°C)	'Warm' end temperature (°C)	$\bar{K}$ (ms^{-1})
2B	Slims Valley Silt	-0.300	0.00	3.00×10^{-13}
1B	" " "	-0.515	+0.075	2.72×10^{-12}
1A	" " "	-0.520	+0.040	3.94×10^{-12}
3A	Castor Silt Loam	-0.300	-0.200	7.04×10^{-13}
3B	" " "	-0.400	-0.200	6.27×10^{-14}
4B	" " "	-0.500	-0.200	9.73×10^{-14}
4D	" " "	-0.600	-0.200	6.44×10^{-14}

*Calculated according to the method outlined in Section 3.7

accuracy in hydraulic conductivity measurements is specified in orders of magnitude. This is due to natural variability. No two samples (even of unfrozen soils) can be expected to give identical values for $\bar{K}$. Add to this the fact that each sample has a different freezing history, then it is hardly surprising that there is not exact agreement between coefficients obtained from different samples. The permeability values presented in Table 4.1 appear to be compatible with data obtained earlier (using the Burt and Williams permeameter) illustrated in Figure 2.4. The curves in Figure 2.4 must be extrapolated to temperatures in the same range as those for the 'cold' end in Table 4.1.

4.5 Results Obtained Using Supercooled Water

Supercooled water has been used successfully in the Burt and Williams isothermal permeameter, and the results are essentially identical to those achieved with lactose solution (see Figure 2.4). Two experiments (Expt. 5 and Expt. 6) were run with the present apparatus, in which supercooled water was present in the end reservoirs instead of lactose solution. Here, unlike the Burt and Williams experiment, there is no external driving force, rather the frozen soil, subjected to a temperature gradient, should act as a kind of pump inducing water migration in the direction of decreasing temperature. Initially, results obtained with supercooled water in the reservoirs appear somewhat surprising, since water moved into the frozen sample at the 'cold' end, and outflow took place from the 'warm' end. In other words, water appeared to be moving

in the opposite direction to the hydraulic gradient implied by the temperature profile. Cumulative inflow and outflow were essentially equal. For example, a temperature gradient of $0.032^{o}C/cm$ across a sample of Castor silt loam soil, at a mean temperature of $-0.2^{o}C$, produced a mean rate of inflow of 6.67×10^{-1} mm^3/min at the 'cold' end, and a mean outflow rate of 7.93×10^{-1} mm^3/min at the 'warm' end (see Figure 4.7). There was no apparent decline in flow rates over the duration of the experiment (6 hours).

Further consideration reveals that this phenomenon should not be so surprising. Since supercooled water is not in thermodynamic equilibrium with the unfrozen soil water, it is to be expected that it will be pulled into the frozen sample. The greatest disparity between potentials exists across the 'cold' end of the sample; thus water moves from the 'cold' reservoir into the frozen soil where ice lensing can be expected to take place. On dismantling the apparatus at the end of Expt. 5 (total duration 4 days), an ice lens, approximately 0.2 cm thick was observed at the 'cold' end of the sample. Presumably a frost heave pressure is generated by the lens growth, causing some melting of ice at the 'warm' end. The subsequent expulsion of water follows directly from the rise in pore water pressure. This hypothesis appears to account for the observed reversal in flow. It is likely that the phenomenon will continue until the ice pressure within the confined sample rises to an equilibrium value. The tendency to 'pull' water into the sample from the 'cold' reservoir should then disappear as the potentials of the supercooled

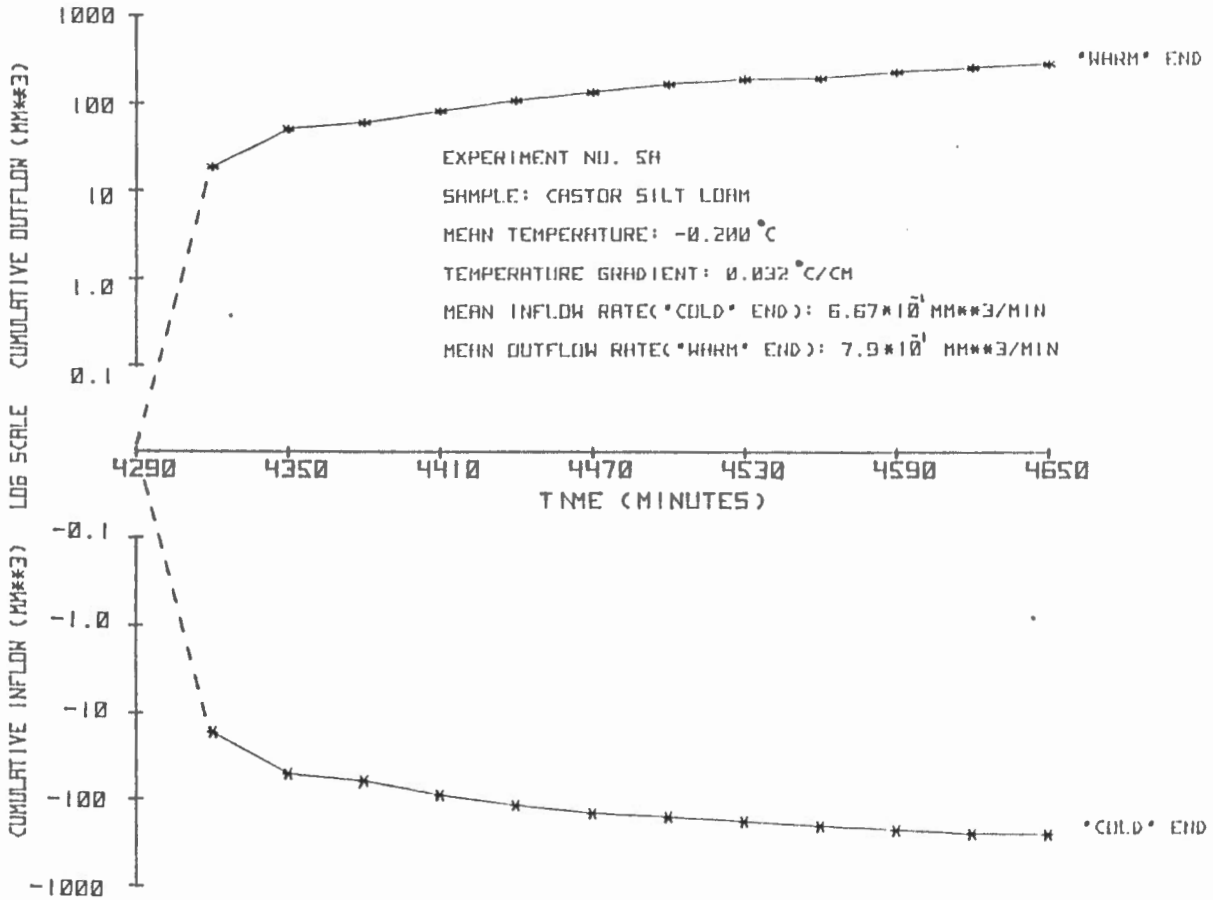

FIGURE 4.7 OBSERVED REVERSAL IN CUMULATIVE INFLOW-OUTFLOW WITH SUPERCOOLED WATER IN THE RESERVOIRS

water and the unfrozen soil water approach a state of mechanical equilibrium.

One test (Expt. 6A) was conducted using a Slims Valley Silt soil in which there was no temperature gradient. Both thermo-electric cooling plates were maintained at a constant temperature of $-0.1^{\circ}C$, while the reservoirs were again filled with supercooled water. According to the explanation developed above, one would expect water to be drawn into the sample from both ends, at least initially. Figure 4.8 however, shows that this was not the case; water continued to move out of the sample from one end, even though there was no apparent gradient of potential. After a period of 6 hours cumulative inflow was observed to be considerably greater than cumulative outflow (54.98 mm^3 compared to 3.04 mm^3). It may be that a very small temperature gradient can exist across the system (i.e. within the limits of measurement precision). If this is the case, then the implied gradient of potential should produce the same effect as that described above. Due to the unstable thermodynamic situation within the frozen sample, the phenomenon may even reverse itself periodically, although there should always be a net inflow, until the ice pressure rises to its equilibrium value.

V THE INFLUENCE OF EXPERIMENTAL PROPERTIES

The experiment demonstrates the movement of water within saturated frozen soils, in response to applied temperature gradients. The inherent properties of the experiment may have significance in relation to rates of

FIGURE 4.8 CUMULATIVE INFLOW-OUTFLOW WITH SUPERCOOLED WATER IN THE RESERVOIRS, AND NO TEMPERATURE GRADIENT ACROSS THE SAMPLE

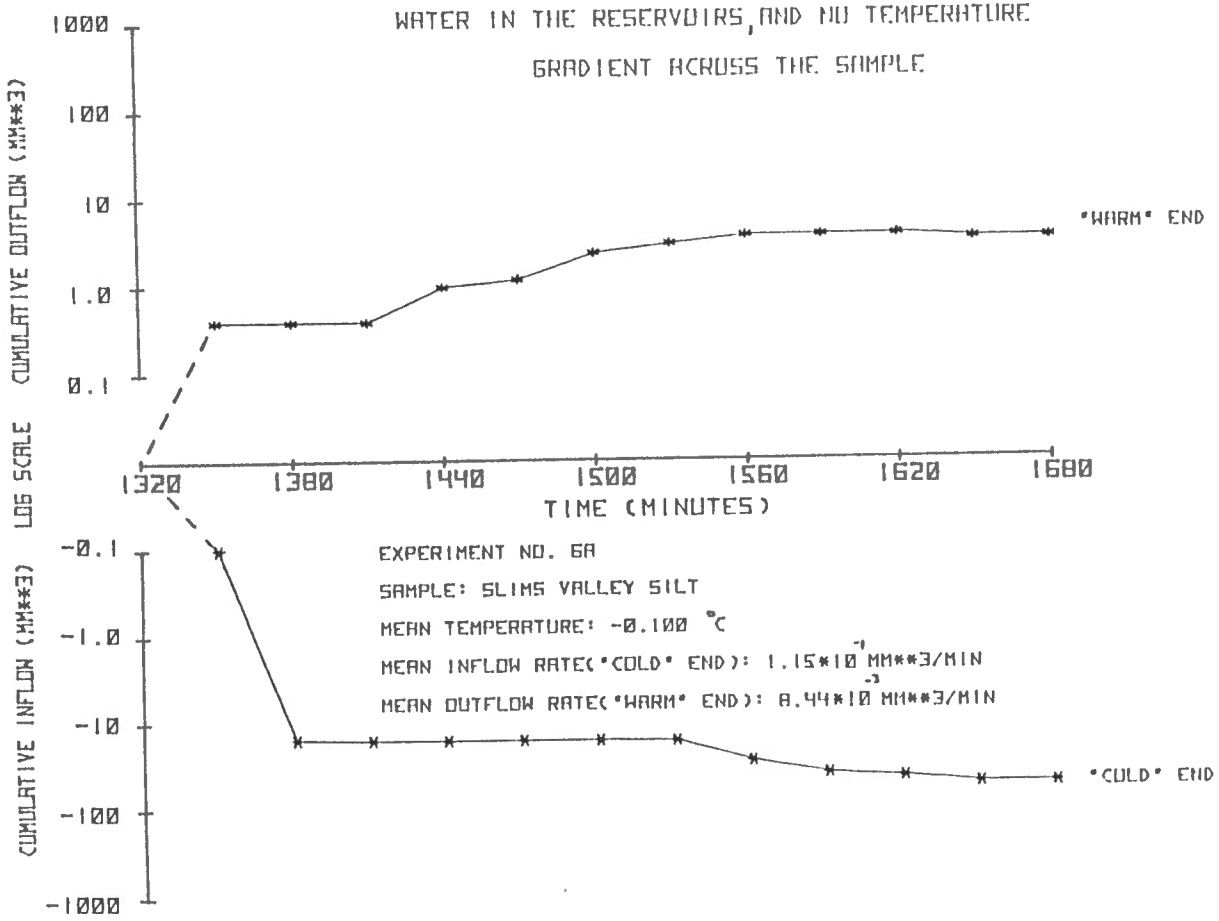

flow which can be expected in the field, or with alternative test procedures. A number of problems result from the experimental design; these are discussed below, with attention being paid to their influence on the results reported in the previous chapter.

5.1 Osmotic Potential Gradients

In most experiments mean rates of inflow were less than the outflow by approximately an order of magnitude (see Appendix III). This implies a net loss of water from the frozen soil sample. In one respect a net gain might be expected since permeability decreases with temperature, non-linearly as in Figure 2.4, while potential decreases linearly, according to Equation 4. Thus, a net inflow could be explained by ice accumulation occurring within the sample. However, several other factors related to the properties of the experiment itself, could account for the observed disparity between inflow and outflow rates:

1. The test procedure adopted involved the use of a single concentration of lactose solution in the end reservoirs. This concentration was such that the potentials of the water in the 'cold' reservoir and the adjacent unfrozen soil water were in equilibrium. Since the same concentration of lactose solution was used in the 'warm' reservoir, the resultant local osmotic potential gradient, coupled with the presence of semi-permeable membranes, could be sufficient to partly or wholely counteract the temperature induced potential gradient at the

'warm' end. Figure 5.1(A) is a schematic representation of the potentials that might be expected to develop in a system with a linear temperature gradient, in which both reservoirs contain similar concentrations of lactose solution. It can be seen that, although the potentials at the 'cold' end are equal, there is a pronounced local osmotic potential gradient across the 'warm' end, equal in magnitude to the total thermal driving potential developed over the whole sample. A decline in observed rates of inflow can be expected on this account. The osmotic potential gradient serves to counteract intake at the 'warm' end, causing an apparent reduction in mean rates of inflow. This is reflected in the cumulative inflow-outflow graphs presented in Chapter 4. These reveal that cumulative inflow is, often one or two orders of magnitude less than cumulative outflow (eg. Expt. 4D), sometimes non-existent (eg. Expt. 3B) and rarely manifested as a cumulative outflow (eg. Expt. 2B). Interpretation of the effects of the counter osmotic potential gradient at the 'warm' end is complicated by the fact that the dialysis membranes are not 100% semi-permeable to the lactose molecules (see next section). The passage of lactose molecules into the soil pores can be expected to weaken the efficiency of the osmotic effect (which depends on the semi-permeability of the membranes), thereby reducing the severity of the counter potential gradient.

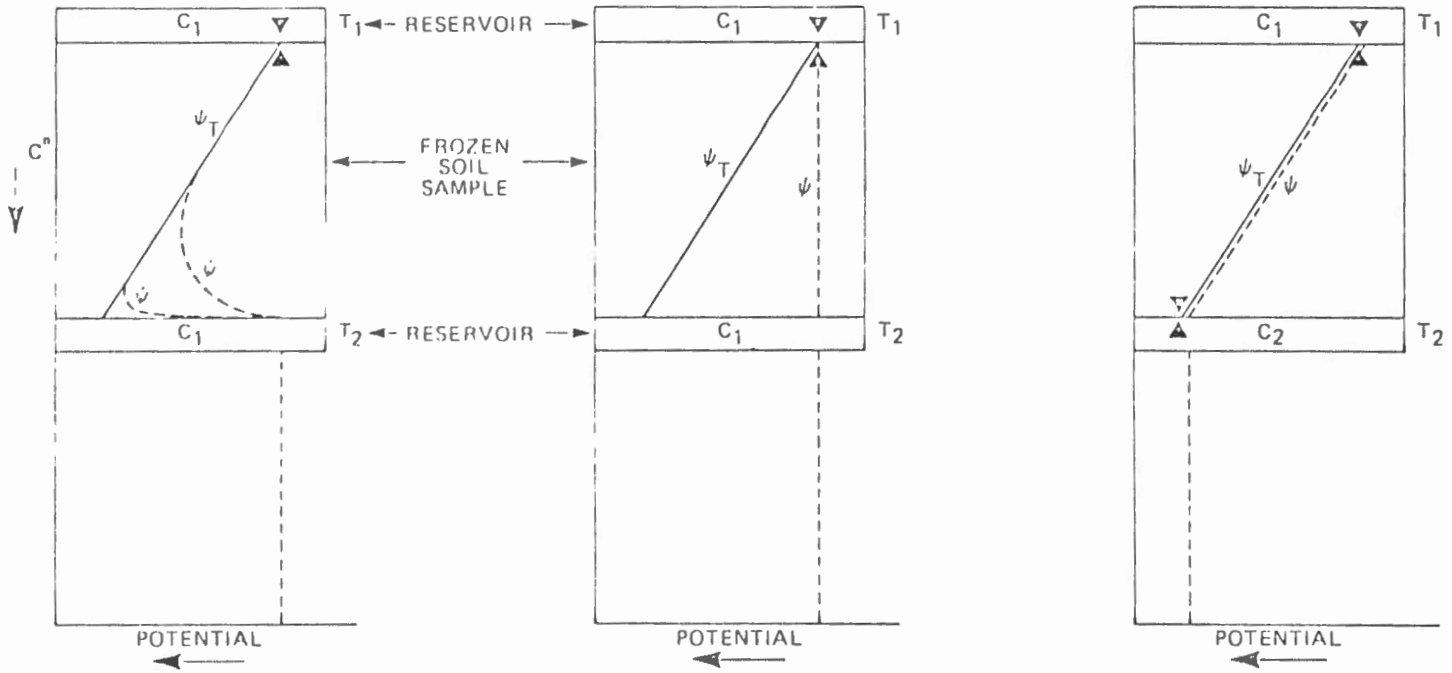

A Initial Situation: pronounced local osmotic potential gradient at the 'warm' end of the sample (i.e. T_2).

B Hypothetical End State: the osmotic potential generated at the 'warm' end cancels out ψ_T to give zero total potential (ψ) across the sample.

C Suggested Situation: with two concentrations of lactose solution (C_1 and C_2) in the reservoirs, no osmotic potential gradient should be generated as long as the temperature gradient exists across the sample.

KEY

T_1 = 'cold' end temperature
T_2 = 'warm' end temperature
C_1 = solute concentration appropriate for T_1
C_2 = solute concentration appropriate for T_2
ψ = total potential; ψ_T = temperature induced hydraulic potential
▽ ▲ = potentials in equilibrium

SCHEMATIC REPRESENTATION OF THE POTENTIALS DEVELOPED WITHIN THE SYSTEM, ASSUMING 100% SEMI-PERMEABLE MEMBRANES

FIGURE 5.1

Depending on the time it takes for the effects of the osmotic potential gradient to be communicated over the entire length of the frozen sample, the system can be expected to approach an end state, as described in Figure 5.1(B). In this case the thermally induced gradient of potential and the osmotic potential gradient cancel each other out; by definition the two must be exactly equal, since the same concentration of lactose solution used in the 'cold' reservoir, was also employed in the 'warm' reservoir. Thus, the total gradient of potential (within the unfrozen soil water) across the length of the sample is equal to zero. As the sample approaches this condition then, one would expect to observe a steady decline in mean rates of inflow and outflow. Eventually flow should stop altogether in accordance with the balance between the two potential gradients. This however, was not the case in any of the tests reported here. For example, Figure 5.2 shows cumulative inflow - outflow measured over the duration of a normal 6 hour experiment (Expt. 1B). The sample used was a Slims Valley Silt soil, subjected to a temperature gradient of $0.0944^{o}C/cm$, with a mean temperature of $-0.220^{o}C$. As might be expected, inflow diminishes to zero with time due to the reverse osmotic potential gradient at the 'warm' end. However, there is no apparent trend towards decreased outflow for the period in which readings were taken.

FIGURE 5.2 THE DISPARITY BETWEEN CUMULATIVE INFLOW-OUTFLOW WITH TIME

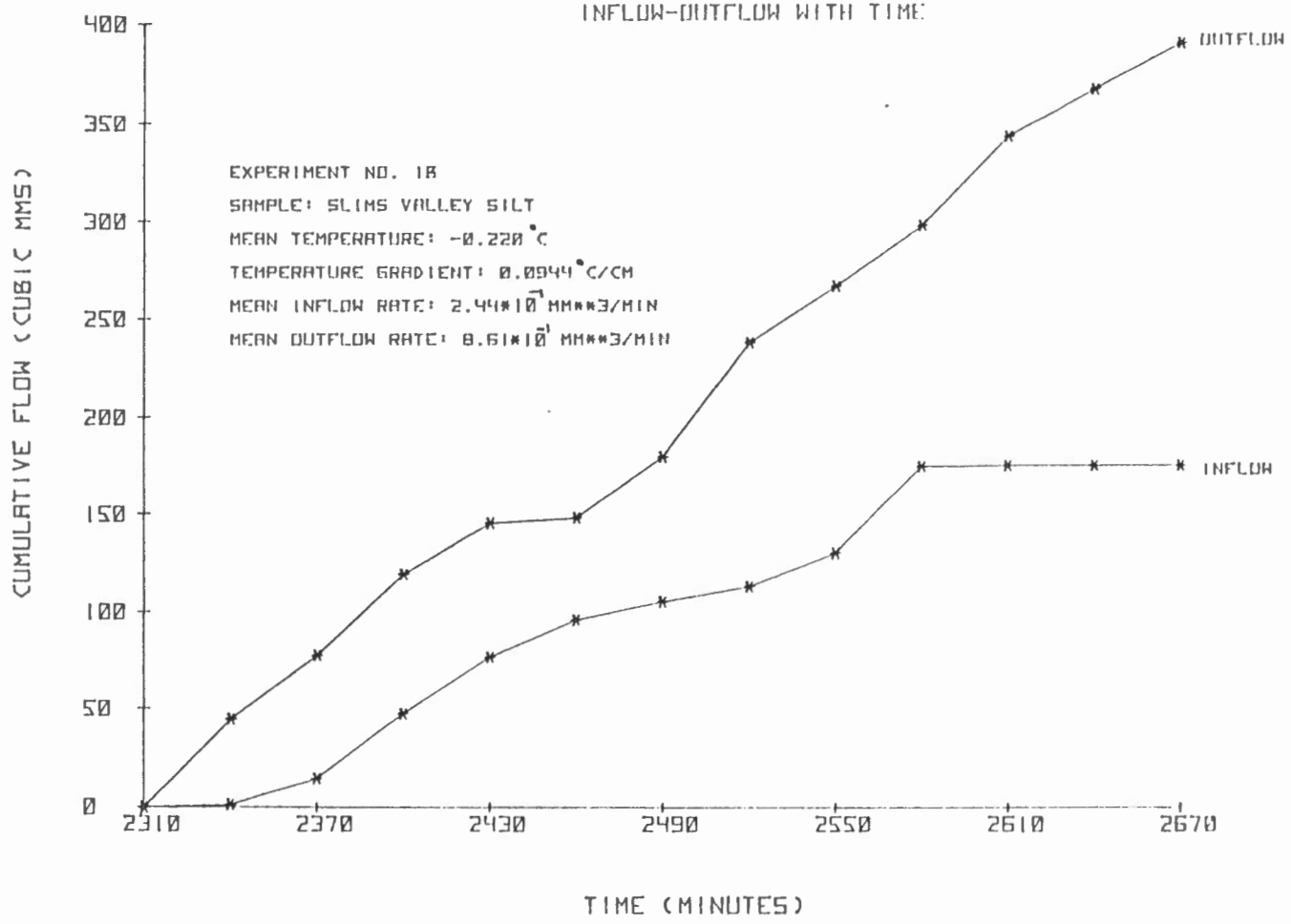

Figure 5.1(C) shows the potential gradients that might be expected to develop in a system with two different concentrations (appropriate for the temperatures of the cooling plates) of lactose solution in the reservoirs. As long as the correct temperature gradient is maintained across the sample, no counter osmotic potential gradient should be generated because the unfrozen water at both ends of the sample is in equilibrium with the two different concentrations of lactose solution in the reservoirs. With such an arrangement, one might expect much higher rates of inflow (due to the absence of the local osmotic potential gradient), so that cumulative inflow exceeds cumulative outflow, the difference being attributable to ice formation within the sample. Outflow rates on the other hand, should be consistent with, or slightly greater than the values achieved in the present study.

2. Water flow into the sample results in a local concentration of lactose in the inflow reservoir; the inverse causes dilution in the outflow reservoir. Thus, an additional osmotic potential gradient is generated over the duration of each test (6 hours). This tends to induce flow in the opposite direction to the gradient of potential implied by the temperature profile; a further decline in flow rates can be expected on this account. The effect is not additive since the reservoirs were flushed with a fresh supply of lactose solution at the beginning of each

experiment.

5.2 Passage of Lactose Molecules Through the Dialysis Membranes

Ideally the solute used in the reservoirs should have large enough molecules not to pass through the semi-permeable membranes at the ends of the frozen sample. However, the small size of the lactose molecules means that they are able to pass, to some extent, through almost any membrane, except those also impermeable to water, which, by definition are unsuitable for this experiment. Gradual movement of lactose molecules into the frozen soil was confirmed by the observation at the end of each experiment of a small thawed layer on both the inflow and outflow faces, normally in the order of 0.3 cm thick, but in extreme cases up to 0.8 cm thick. The problem increases with time, and for this reason tests were usually terminated after a period of two or three days.

The passage of lactose into the soil capillaries adds an osmotic potential which further lowers the freezing point of the unfrozen soil water. Consequently, some melting of ice can be expected to occur, which will result in an increase in the permeability of the thawed part of the sample. According to Burt and Williams (1976) however, the observed agreement when carbowax (Polyethelyene Glycol) and lactose were interchanged in an experiment with Leda clay indicates that the diffusion of the lactose has only a "minimal effect" on flow rates, and thus hydraulic conductivity determinations.

The thawed sections of the sample can be expected to have a much

higher permeability compared with that of the frozen soil. However, rates of flow will continue to be determined by the lower conductivities of the frozen portion, regardless of the presence of the unfrozen layers. In calculating hydraulic conductivity values a simple correction must be made for the presence of the thawed layers; the path length of flow L, is taken to be the length of the sample remaining frozen at the end of each experiment.

Notwithstanding thawed layers at both ends of the sample, it seems reasonable to attribute the observed outflow to moisture migration occurring within the frozen soil. The relationship between temperature and free energy (Equation 4) does not apply above $0^{o}C$; consequently thermal gradients in unfrozen soil do not induce the same potential for water movement. It follows that the observed fluxes were most likely due to migration of water within the remaining frozen portion of the sample. Although the passage of lactose molecules into the frozen soil detracts from the theoretical beauty of the experiment, the above evidence seems to indicate that the phenomenon is of little practical import.

5.3 Pressures Generated Within the Sample Container

The possible build-up of frost heave pressures within the sample container must be taken into account, in any interpretation of the fluxes observed. Ice lensing, taking place towards the colder end may give rise to an increase in the frost heave pressures generated within the confined sample. The subsequent rise in pore-water pressures may be sufficient to

counteract intake and reduce observed rates of inflow. Obviously further research is needed on this point. Time did not permit detailed investigations of the post heave pressures generated within the sample container. Modification of the present apparatus should include the construction of an attachment to facilitate the precise measurement of pressures generated by the water migration process.

5.4 Error Analysis

The calculated rates of flow should be placed into some perspective as to their degree of accuracy. This involves consideration of the accuracy of each individual measurement used in the computation of the flow rates. The length and radius of the plexiglass sample container were known to within 0.0025 cm. Both capillary tubes were determined to have radii of 0.025 cm, with confidence limits of $\pm$ 0.002 cm. Similarly, timing the movement of menisci along the capillary tubes using a scale in conjunction with a magnifying glass and stopwatch was also very accurate. Perhaps the greatest source of error lies in the volumes of water contained in the connecting tubes; the following effects may have been responsible for some degree of variation:

1. The flexibility of the 'tygon' tubing used to connect the capillary tubes to the inflow-outflow reservoirs, introduces the possibility of volume changes occurring, other than those associated with water entering or leaving the frozen sample. Expansion or contraction of these tubes, for whatever reason

(eg. thermally induced or even accidental squeezing) will be translated into a positive or negative movement of the menisci in the capillary tubes. Such variance could produce a significant error, especially when one compares the total volume of water contained in the connecting tubes (approximately 9.65 cm^3) with the extremely small volumes of inflow and outflow being measured.

2. A small change in volume may occur as a result of air coming out of solution, in response to an increase in ambient temperature. This phenomenon can be expected to take place where the 'tygon' tubing passes out of the incubator (maintained at a mean temperature of $0^{\circ}C$) into air at room temperature; indeed air bubbles were commonly observed at this junction. The volume changes associated with a build up of air bubbles are likely to be only very small, but they may be sufficient to register in the capillary tubes as a slight positive movement of the menisci. Such movements might serve to accentuate outflow rates and cause an apparent decline in observed rates of inflow.

The thermistors were calibrated in a refrigerated 'Hotpack' bath circulator, against a mercury in glass thermometer, with a certified accuracy of $\pm$ $0.01^{\circ}C$ (N.R.C. calibration report No. APH 2173). Since the same thermistors were used for all the experiments, the relative differences between the recorded temperatures remained constant. The accuracy of the temperature measurements implies confidence limits of approximately $\pm$ $0.1245 \times 10^5 Nm^{-2}$ (or 124.5 cm of water head) when interpolating gradients

of potential from the temperature profiles. This is a relatively small error (always less than 10%) when one considers the size of the heads induced by the applied thermal gradients. It is impossible to quantify the cumulative error ensuing from all these effects. In all likelihood however, the value will be considerable in absolute terms, but when viewed in the context of orders of magnitude (which this experiment is concerned with), it is probably quite small.

VI SUMMARY AND CONCLUSIONS

1. Apparatus and procedures for the direct measurement of thermally actuated water migration in saturated, frozen soils have been developed. The experimental configuration was similar to that used by Burt and Williams (1976), the fundamental difference being that the hydraulic gradient was induced by a gradient of temperature rather than by a pressure differential. The frozen soil sample and reservoirs were sandwiched between two Peltier modules, controlled by a thermo-electric cooling control system. The reservoirs were normally filled with lactose solution, although supercooled water was used for two experiments. When a stable, linear temperature gradient was established across the system, water appeared to pass from the 'warm' reservoir into the frozen sample, and out into the second, colder reservoir.

2. Results obtained from the experiments have been examined with regard to current theoretical and applied studies of frozen ground. It is well known that frozen soils contain significant amounts of unfrozen water coexisting with the ice phase. This water has a potential relative to

pure, bulk water, which is lower by an amount increasing as the temperature decreases. Thus, a temperature gradient in frozen soil implies a flux of water in the direction of decreasing temperature, at a rate dependent on the permeability in the frozen state.

3. Fluxes were seen to vary, regardless of soil type, with the temperature gradient (i.e. the potential for water movement) and the mean temperature of the frozen sample (i.e. the apparent hydraulic conductivity). Observed rates of flow ranged from 10^{-1} to 10^{-3} mm^3/min. These values are consistent with conductivity coefficients for frozen soils (at similar temperatures) measured earlier. Two soils were used for all the tests; since these had similar pore size distributions it proved impossible to identify variations in flow rate caused by soil type.

4. With supercooled water in the reservoirs, flow appeared to take place in the opposite direction to the hydraulic gradient implied by the temperature profile. A hypothesis was developed explaining this phenomenon in terms of the pressures generated by the water migration process.

5. The data have some shortcomings, which came to light as the experiments progressed. The problem of reverse osmotic potential gradients in particular, complicates analysis of the results. The inherent properties of the test procedure adopted, could have significance with respect to rates of flow that might be expected in the field or with alternative experimental arrangements.

6. The possible build-up of frost-heave pressures within the sample container should be taken into account in any interpretation of the observed

fluxes. However, time did not permit detailed investigation of this phenomenon.

7. Although analysis of the results is made difficult by the complex thermodynamic situation, and the number of variables involved, the experiments as a whole demonstrate the migration of water within frozen soils, in response to temperature gradients. The apparatus should not be viewed strictly as a permeameter, rather the frozen soil, subjected to a temperature gradient acts as a kind of pump, inducing water migration in the direction of decreasing temperature. Calculation of hydraulic conductivity coefficients is possible using the Darcy Equation, but the apparatus is perhaps best regarded as providing a novel approach to conventional frost-heaving experiments.

6.1 Suggestions for Future Research

Modification should include monitoring the frost heave pressures generated within the sample container. Volume changes should be measureable, via an expansive, impermeable rubber membrane fitted over the outflow face of the sample, either with a pressure transducer or through displacement of liquid from the outflow reservoir. The application of counter-pressures on the outflow reservoir, sufficient to stop flow, would provide an indication in mechanical terms, of the temperature induced driving forces. Improvement of the test procedure should involve the use of two different concentrations of lactose solution (corresponding to the temperatures of the cooling plates) in the reservoirs, for each temperature gradient

investigated. Clarification of the influence of soil type on flow rates, awaits the testing of a large number of different soils, for which unfrozen water contents and grain size distributions are known.

BIBLIOGRAPHY

Aitchison, G.D., K. Russam and B.G. Richards, 1966, "Engineering concepts of moisture equilibria and moisture changes in soils", Road Res. Lab., Rept. 38, Min. of Transp. (U.K.), 36 pp.

Anderson, D.M., 1968, "Undercooling, freezing point depression, and ice nucleation of soil water", Israel J. Chem., 22, pp. 349-355.

Anderson, D.M., and P. Hoekstra, 1965, "Migration of inter-lamellar water during freezing and thawing of Wyoming bentonite", Soil Sci. Soc. Am. Proc., 29, pp. 498-504.

Anderson, D.M. and N.R. Morgenstern, 1973, "Physics, chemistry and mechanics of frozen ground: A Review", In: Permafrost, 2nd Int. Conf., North American Contributions, Nat. Acad. Sci., Washington D.C., pp. 257-288.

Bouyoucos, G.J., 1916, "The freezing point method as a new means of measuring the concentration of the soil solution directly in the Soil", Mich. Agric. Exp. Sta. Bull, 24, pp. 1-44.

Burt, T.P., 1974, "A Study of hydraulic conductivity in frozen soils", Unpublished M.A. Thesis, Carleton University, Ottawa, 85 pp.

Burt, T.P., and P.J. Williams, 1976, "Hydraulic conductivity in frozen soils", Earth Surface Processes, 1, pp. 349-360.

Edlefsen, N.E., and A.B.C. Anderson, 1943, "Thermodynamics of Soil Moisture", Hilgardia, 15, pp. 31-298.

Harlan, R.L., 1973, "An analysis of coupled heat-fluid transport in partially frozen soil", Water Resour. Res., 9, pp. 314-1323.

Harlan, R.L., 1974, "Dynamics of water movement in permafrost: A Review", Proc. Workshop Seminar Permafrost Hydrol., Can. Nat. Com., Int. Hydrol., pp. 69-77.

Hoekstra, P., 1966, "Moisture movement in soils under temperature gradients with the cold-side temperature below freezing", Water Resour. Res., 2, pp. 241-250.

Hoekstra, P., 1969, "Water movement and freezing pressures", Soil Sci. Soc. Am. Proc., 33, pp. 512-518.

Koopmans, R.W.R., and R.D. Miller, 1966, "Soil freezing and soil water characteristic curves", Soil Sci. Soc. Am. Proc., 30, pp. 680-685.

Mackay, J.R., J. Ostrick, C.P. Lewis, and D.K. Mackay, 1979, "Frost heave at ground temperatures below 0°C, Inuvik, Northwest Territories", Sci. Tech. Notes in Current Res. Part A., Geol. Surv. Can., Paper 79-1A, pp. 403-405.

Miller, R.D., 1970, "Ice Sandwich: Functional semipermeable membrane", Science, 169, pp. 584-585.

Miller, R.D., J.P.G. Loch, and E. Bresler, 1975, "Transport of water and heat in a frozen permeameter", Soil Sci. Soc. Am. Proc., 39, pp. 1029-1036.

Nersesova, Z.A., and N.A. Tsytovich, 1966, "Unfrozen water in frozen soils" In: Permafrost, Proc. 1st Int. Conf., Nat. Acad. Sci., Washington D.C., pp. 230-234.

Nye, J.F., and F.C. Frank, 1973, "Hydrology of the intergranular veins in a temperate glacier", Publ. No. 95, Int. Assoc. Sci. Hydrol.

Osterkamp, T.E., 1975, "Structure and properties of ice lenses in frozen ground", Proc. Conf. Soil Water Problems in Cold Regions, Calgary, pp. 89-111.

Rose, C.W., 1966, "Agricultural Physics", Pergamon Press, Oxford, 230 pp.

Schofield, R.K., 1935, "The PF of the water in soil", 3rd Int. Cong. Soil Sci., 2, pp. 37-48.

Taylor, D.W., 1949, "Fundamentals of soil mechanics", Wiley, New York, 700 pp.

Williams, P.J., 1967, "Properties and behaviour of freezing soils", Norwegian Geotechnical Inst., Publ. No. 72, 120 pp.

Williams, P.J., 1968, "Thermoelectric cooling for precise temperature control of frozen and unfrozen soils", Can. Geotech. Journ., 5, pp. 264-266.

Williams, P.J., 1976, "Volume change in frozen soils", Laurits Bjerrum Memorial Vol., Norw. Geotechn. Inst., pp. 233-246.

Williams, P.J., 1977, "Thermodynamic conditions for ice accumulation in freezing soils", In: Proc. Int. Symp. on Frost Action in Soils, University of Lulea, Sweden, 1, pp. 42-53.

Williams, P.J., and E. Perfect, 1979, "Investigation of rates of water movement through frozen soils", Final Report for the Department of Energy, Mines and Resources, Earth Physics Branch, Ottawa, DSS File No. ISU77-00269, 36 pp.

APPENDIX I

SCALE DRAWING OF THE EXPERIMENTAL APPARATUS

FIGURE 1.1

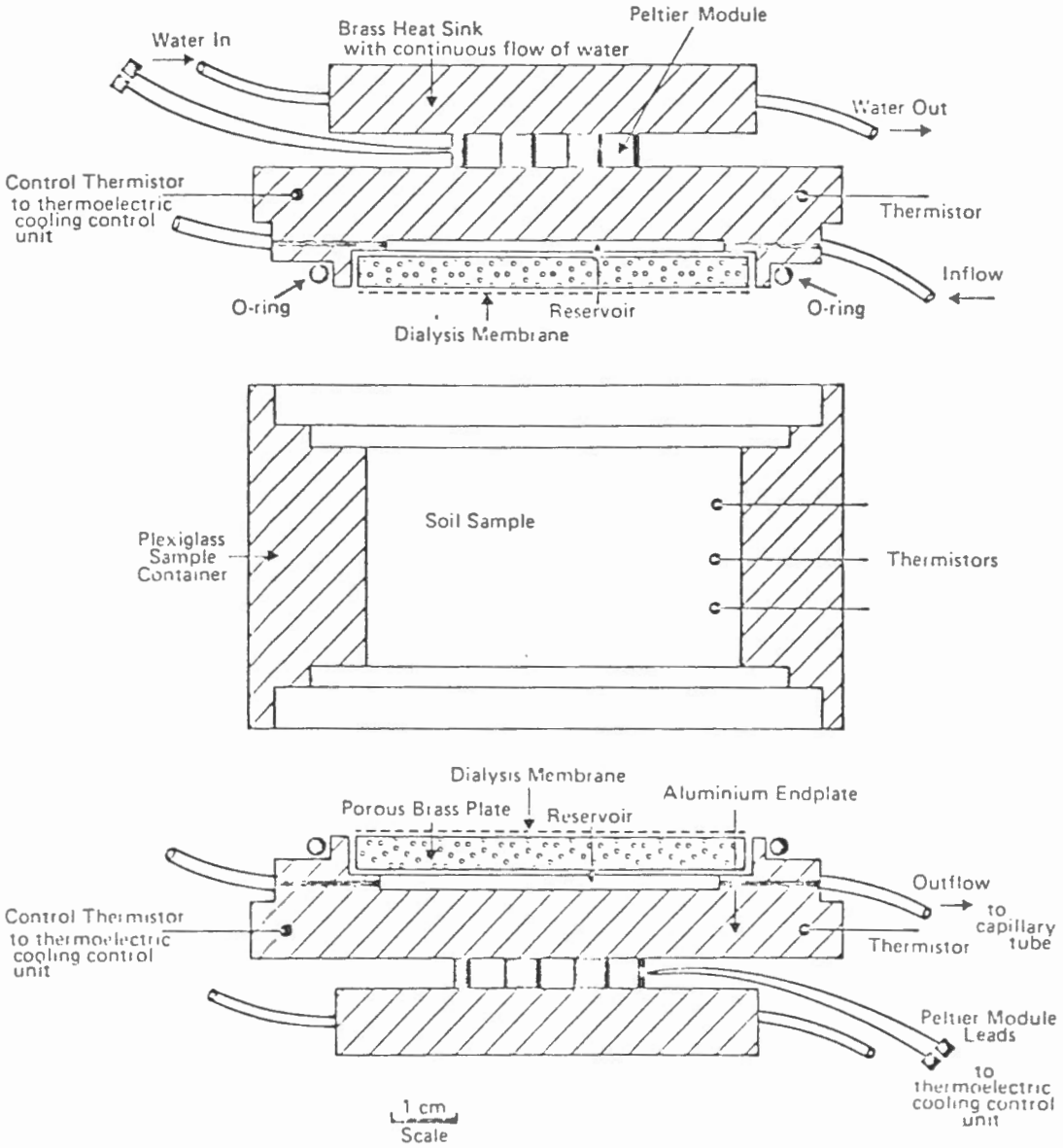

CROSS-SECTION OF THE EXPERIMENTAL APPARATUS.

APPENDIX II

FREEZING POINT DEPRESSION, $\Delta^{o}C$, AS A FUNCTION OF LACTOSE CONCENTRATION

Reference: "CRC Handbook of Chemistry and Physics", Page D-218.

LACTOSE, $C_{12}H_{22}O_{11} \cdot 1H_2O$

Molecular weight = 342.30

Formula weight = 360.31

Anhydrous Solute Concentration g/l	Molar Concentration g-mol/l	Freezing Point Depression $\Delta\,^{o}C$
0.50	5.0	0.027
1.00	10.0	0.055
1.50	15.1	0.083
2.00	20.1	0.112
2.50	25.2	0.140
3.00	30.3	0.169
3.50	35.4	0.198
4.00	40.6	0.228
4.50	45.7	0.258
5.00	50.9	0.288
5.50	56.1	0.319
6.00	61.4	0.351
6.50	66.6	0.385
7.00	71.9	0.420
7.50	77.2	0.456
8.00	82.5	0.495
8.50	87.8	No value given
9.00	93.1	" " "
9.50	98.5	" " "
10.00	103.9	" " "

APPENDIX III

A RECORD OF RESULTS OBTAINED

Note: Prefrozen samples were used throughout. The estimated limit of accuracy for temperature measurements was $\pm 0.01^{o}C$. Thermister code:

T_1 - End Plate temperature ("cold")

T_2 - Temperature of sample 2.30 cms from T_1

T_3 - Temperature of sample 3.15 cms from T_1

T_4 - Temperature of sample 4.00 cms from T_1

T_5 - End Plate temperature ("warm"), 6.25 cms from T_1

All experiments were conducted using lactose solution in the reservoirs, except for numbers 5 and 6 where supercooled water was used. Flow normally occured in the direction of decreasing temperature, outflow taking place from the "cold" end (T_1) and inflow at the "warm" end (T_5). Outflow is considered positive, and inflow negative. A positive sign in the inflow column denotes outflow from the "warm" end, and a negative sign in the outflow column denotes inflow at the "cold" end. All moisture contents are expressed as per cent dry weight.

EXPERIMENT NO. 1A, SLIMS VALLEY SILT

Time Interval (Min)	Temperature Gradient (°C)					Meniscus* (Distance travelled, mm)		Cumulative Flow (mm^3)	
	T_1	T_2	T_3	T_4	T_5	Inflow (-ve)	Outflow (+ve)	Inflow (-ve)	Outflow (+ve)
840-870	-0.520/ -0.525	-0.365/ -0.380	-0.220/ -0.235	-0.080/ -0.085	+0.040/ +0.055	2.0	0.5	0.39	0.10
870-900	-0.530	-0.390	-0.250	-0.090	+0.055	0.5	2.5	0.49	0.39
900-930	-0.535	-0.400	-0.260	-0.100	+0.055	0.0	4.0	0.49	1.18
930-960	-0.540	-0.405	-0.265	-0.105	+0.050	2.5	63.0	0.98	13.55
960-990	-0.540	-0.405	-0.265	-0.105	+0.050	16.0	72.5	4.12	27.79
990-1020	-0.540	-0.405	-0.270	-0.100	+0.055	79.0	108.5	19.64	49.09
1020-1050	-0.515	-0.380	-0.240	-0.075	+0.080	1.0	113.0	19.83	71.28
1050-1080	-0.515	-0.375	-0.240	-0.075	+0.080	0.0	207.5	19.83	112.03
1080-1110	-0.510	-0.375	-0.235	-0.070	+0.075	0.5	235.0	19.93	158.18
1110-1140	-0.515	-0.370	-0.235	-0.070	+0.080	0.0	239.0	19.93	205.11
1140-1170	-0.510	-0.375	-0.235	-0.070	+0.080	0.0	244.0	19.93	253.03
1170-1200	-0.505	-0.375	-0.240	-0.070	+0.080	0.0	209.0	19.93	294.07

*Radius of capillary tube = 0.025 cm

Initial Water Content: 29.01%
Temperature Gradient: 0.0896°C/cm
Mean Temperature: -0.240°C
Inflow Rate (Mean): 8.27×10^{-2} $mm^3 min^{-1}$, for period 840-1500 min
Outflow Rate (Mean): 5.77×10^{-1} $mm^3 min^{-1}$, for period 840-1500 min

EXPERIMENT NO. 1B, SLIMS VALLEY SILT

Time Interval (Min)	Temperature Gradient (^{o}C)					Meniscus* (Distance travelled, mm)		Cumulative Flow (mm^3)	
	T_1	T_2	T_3	T_4	T_5	Inflow (-ve)	Outflow (+ve)	Inflow (-ve)	Outflow (+ve)
2310-2340	-0.530/ -0.515	-0.400/ -0.370	-0.255/ -0.255	-0.105/ -0.065	+0.035/ +0.075	6.0	228.5	1.18	44.87
2340-2370	-0.515	-0.375	-0.230	-0.070	+0.080	66.5	168.5	14.24	77.96
2370-2400	-0.515	-0.380	-0.235	-0.075	+0.080	169.0	213.0	47.43	119.79
2400-2430	-0.515	-0.380	-0.235	-0.070	+0.075	150.0	134.0	76.88	146.10
2430-2460	-0.515	-0.380	-0.240	-0.075	+0.075	97.5	13.0	96.03	148.66
2460-2490	-0.520	-0.380	-0.240	-0.070	+0.085	47.0	161.5	105.26	180.37
2490-2520	-0.515	-0.390	-0.250	-0.085	+0.070	39.5	296.5	113.01	238.60
2520-2550	-0.520	-0.390	-0.250	-0.090	+0.070	88.0	148.0	130.30	267.66
2550-2580	-0.515	-0.385	-0.250	-0.085	+0.070	228.0	160.0	175.07	299.08
2580-2610	-0.515	-0.385	-0.250	-0.085	+0.070	3.0	231.5	175.66	344.54
2610-2640	-0.515	-0.385	-0.250	-0.090	+0.070	0.0	122.5	175.66	368.60
2640-2670	-0.515	-0.385	-0.255	-0.090	+0.070	0.0	118.0	175.66	391.77

*Radius of capillary tube = 0.025 cm

Initial Water Content: 29.01%
Temperature Gradient: $0.0944^{o}C/cm$
Mean Temperature: $-0.220^{o}C$
Inflow Rate (Mean): 2.44×10^{-1} $mm^3 min^{-1}$, for period 2310-3030 min
Outflow Rate (Mean): 8.61×10^{-1} $mm^3 min^{-1}$, for period 2310-3030 min

EXPERIMENT NO. 2A, SLIMS VALLEY SILT

Time Interval (Min)	Temperature Gradient (°C)					Meniscus* (Distance travelled, mm)		Cumulative Flow (mm^3)	
	T_1	T_2	T_3	T_4	T_5	Inflow (-ve)	Outflow (+ve)	Inflow (-ve)	Outflow (+ve)
1230-1260	-0.320/ -0.320	-0.375/ -0.375	-0.350/ -0.350	-0.315/ -0.315	-0.320/ -0.320	0.0	0.0	0.00	0.00
1260-1290	-0.325	-0.375	-0.355	-0.320	-0.330	0.0	0.0	0.00	0.00
1290-1320	-0.320	-0.380	-0.355	-0.320	-0.325	0.0	0.0	0.00	0.00
1320-1350	-0.325	-0.380	-0.355	-0.320	-0.335	0.0	0.0	0.00	0.00
1350-1380	-0.310	-0.375	-0.355	-0.315	-0.320	0.0	1.0	0.00	0.20
1380-1410	-0.325	-0.380	-0.350	-0.315	-0.330	0.0	0.5	0.00	0.29
1410-1440	-0.325	-0.375	-0.350	-0.315	-0.330	0.0	0.5	0.00	0.39
1440-1470	-0.315	-0.375	-0.350	-0.310	-0.325	0.0	0.5	0.00	0.49
1470-1500	-0.315	-0.370	-0.345	-0.310	-0.320	0.0	1.5	0.00	0.79
1500-1530	-0.320	-0.370	-0.345	-0.310	-0.330	0.0	1.0	0.00	0.98
1530-1560	-0.315	-0.365	-0.345	-0.310	-0.320	0.0	0.5	0.00	1.08
1560-1590	-0.325	-0.370	-0.340	-0.310	-0.330	0.0	0.5	0.00	1.18

*Radius of capillary tube = 0.025 cm

Initial Water Content: 24.29%
Temperature Gradient: 0.00°C/cm
Mean Temperature: 0.3275°C
Inflow Rate (Mean): 0.00 $mm^3 min^{-1}$, for period 1050-1770 min
Outflow Rate (Mean): 1.64×10^{-3} $mm^3 min^{-1}$, for period 1050-1770 min

EXPERIMENT NO. 2B, SLIMS VALLEY SILT

Time Interval (Min)	Temperature Gradient (°C)					Meniscus* (Distance travelled, mm)		Cumulative Flow (mm^3)	
	T_1	T_2	T_3	T_4	T_5	Inflow (-ve)	Outflow (+ve)	Inflow (-ve)	Outflow (+ve)
2460-2490	-0.300/ -0.325	-0.255/ -0.260	-0.170/ -0.175	-0.080/ -0.085	-0.005/ 0.000	+22.0	3.0	+ 4.32	0.59
2490-2520	-0.335	-0.265	-0.180	-0.090	-0.010	+ 10.0	0.5	+ 6.28	0.69
2520-2550	-0.325	-0.265	-0.185	-0.090	+0.010	+ 6.5	0.5	+ 7.56	0.79
2550-2580	-0.320	-0.270	-0.185	-0.090	+0.015	+ 0.5	2.0	+ 7.66	1.18
2580-2610	-0.340	-0.270	-0.185	-0.090	+0.015	+ 4.0	0.5	+ 8.44	1.28
2610-2640	-0.325	-0.270	-0.185	-0.090	+0.005	+ 10.0	3.0	+ 10.41	1.87
2640-2670	-0.320	-0.270	-0.190	-0.090	+0.005	+ 96.5	1.5	+ 29.36	2.16
2670-2700	-0.320	-0.270	-0.185	-0.090	0.000	0.0	46.5	+ 29.36	11.29
2700-2730	-0.315	-0.270	-0.185	-0.090	0.000	+ 0.5	3.0	+ 29.46	11.88
2730-2760	-0.320	-0.270	-0.185	-0.090	+0.010	+ 170.0	44.0	+ 62.84	20.52
2760-2790	-0.320	-0.270	-0.185	-0.090	+0.015	+ 1.0	91.5	+ 63.04	38.49
2790-2820	-0.320	-0.265	-0.185	-0.090	0.000	+ 1.0	2.5	+ 63.23	38.98

*Radius of capillary tube = 0.025 cm

Initial Water Content: 24.29%
Temperature Gradient: 0.0512°C/cm
Mean Temperature: -0.160°C
Inflow Rate (Mean): $+2.26 \times 10^{-1}$ $mm^3 min^{-1}$, for period 2460-3180 min
Outflow Rate (Mean): 9.85×10^{-2} $mm^3 min^{-1}$, for period 2460-3180 min

EXPERIMENT NO. 3A, CASTOR SILT LOAM

Time Interval (Min)	Temperature Gradient (^{o}C)					Meniscus* (Distance travelled, mm)		Cumulative Flow (mm^3)	
	T_1	T_2	T_3	T_4	T_5	Inflow (-ve)	Outflow (+ve)	Inflow (-ve)	Outflow (+ve)
2460-2490	-0.300/ -0.300	-0.260/ -0.280	-0.210/ -0.220	-0.185/ -0.190	-0.200/ -0.200	0.0	1.0	0.00	0.20
2490-2520	-0.305	-0.280	-0.225	-0.190	-0.205	0.0	0.5	0.00	0.29
2520-2550	-0.300	-0.280	-0.230	-0.195	-0.200	0.5	0.5	0.10	0.39
2550-2580	-0.305	-0.280	-0.230	-0.195	-0.200	1.0	0.0	0.29	0.39
2580-2610	-0.300	-0.285	-0.230	-0.195	-0.200	0.0	8.0	0.29	1.96
2610-2640	-0.305	-0.285	-0.230	-0.195	-0.200	0.5	1.0	0.39	2.16
2640-2670	-0.300	-0.285	-0.230	-0.195	-0.200	0.5	13.5	0.49	4.81
2670-2700	-0.300	-0.285	-0.230	-0.195	-0.195	0.0	0.0	0.49	4.81
2700-2730	-0.300	-0.280	-0.230	-0.195	-0.200	0.5	22.0	0.59	9.13
2730-2760	-0.305	-0.285	-0.230	-0.195	-0.205	0.0	2.0	0.59	9.52
2760-2790	-0.305	-0.280	-0.230	-0.195	-0.205	0.0	10.5	0.59	11.59
2790-2820	-0.300	-0.285	-0.230	-0.195	-0.200	14.0	11.0	3.34	13.75

*Radius of capillary tube = 0.025 cm

Initial Water Content: 47.87%
Temperature Gradient: $0.016^{o}C/cm$
Mean Temperature: $-0.250^{o}C$
Inflow Rate (Mean): $9.27 \times 10^{-3}\ mm^3 min^{-1}$
Outflow Rate (Mean): $3.82 \times 10^{-2}\ mm^3 min^{-1}$

EXPERIMENT NO. 3B, CASTOR SILT LOAM

Time Interval (Min)	Temperature Gradient (°C)					Meniscus* (Distance travelled, mm)		Cumulative Flow (mm^3)	
	T_1	T_2	T_3	T_4	T_5	Inflow (-ve)	Outflow (+ve)	Inflow (-ve)	Outflow (+ve)
3960-3990	-0.400/ -0.400	-0.355/ -0.355	-0.285/ -0.280	-0.230/ -0.230	-0.200/ -0.200	0.0	2.5	0.00	0.49
3990-4020	-0.400	-0.360	-0.285	-0.230	-0.195	0.0	6.5	0.00	1.77
4020-4050	-0.400	-0.355	-0.285	-0.230	-0.200	0.0	1.0	0.00	1.96
4050-4080	-0.400	-0.355	-0.285	-0.235	-0.205	0.0	1.5	0.00	2.26
4080-4110	-0.400	-0.355	-0.285	-0.230	-0.200	0.0	1.0	0.00	2.45
4110-4140	-0.405	-0.355	-0.285	-0.235	-0.210	0.0	0.5	0.00	2.55
4140-4170	-0.400	-0.355	-0.280	-0.230	-0.200	0.0	3.0	0.00	3.14
4170-4200	-0.400	-0.355	-0.285	-0.235	-0.200	0.0	1.5	0.00	3.44
4200-4230	-0.405	-0.360	-0.285	-0.230	-0.205	0.0	3.5	0.00	4.12
4230-4260	-0.400	-0.355	-0.285	-0.230	-0.200	0.0	2.0	0.00	4.52
4260-4290	-0.400	-0.355	-0.285	-0.230	-0.200	0.0	1.0	0.00	4.71
4290-4320	-0.400	-0.355	-0.280	-0.230	-0.205	0.0	1.0	0.00	4.91

*Radius of capillary tube = 0.025 cm

Initial Water Content: 47.87%
Temperature Gradient: 0.032°C/cm
Mean Temperature: -0.300°C
Inflow Rate (Mean): 0.00 $mm^3 min^{-1}$
Outflow Rate (Mean): 1.36×10^{-2} $mm^3 min^{-1}$

EXPERIMENT NO. 4A, CASTOR SILT LOAM

Time Interval (Min)	Temperature Gradient (°C)					Meniscus* (Distance travelled, mm)		Cumulative Flow (mm^3)	
	T_1	T_2	T_3	T_4	T_5	Inflow (-ve)	Outflow (+ve)	Inflow (-ve)	Outflow (+ve)
0-30	-0.500/ -0.500	-0.125/ -0.145	-0.095/ -0.115	-0.060/ -0.080	-0.205/ -0.205	-	-	-	-
30-60	-0.500	-0.165	-0.115	-0.090	-0.205	+389.5	25.5	+76.49	5.01
60-90	-0.500	-0.185	-0.085	-0.050	-0.205	+330.0	48.0	+141.29	14.43
90-120	-0.500	-0.230	-0.105	-0.065	-0.200	+250.0	34.0	+190.39	21.11
120-150	-0.500	-0.265	-0.115	-0.070	-0.200	+188.5	61.0	+227.40	33.09
150-180	-0.500	-0.290	-0.125	-0.075	-0.205	+241.0	12.0	+274.73	35.45
180-210	-0.500	-0.310	-0.140	-0.080	-0.200	+203.0	19.5	+314.60	39.28
210-240	-0.500	-0.325	-0.155	-0.085	-0.200	+5.0	44.0	+315.58	47.92
240-270	-0.505	-0.340	-0.170	-0.095	-0.200	+5.5	5.5	+316.66	49.00
270-300	-0.505	-0.355	-0.185	-0.105	-0.200	+5.0	1.5	+317.64	49.30
300-330	-0.500	-0.360	-0.195	-0.110	-0.200	+290.5	6.0	+374.68	50.47
330-360	-0.500	-0.370	-0.210	-0.125	-0.205	+118.0	108.5	+397.86	71.78

*Radius of capillary tube = 0.025 cm

Initial Water Content: 41.33%
Temperature Gradient: 0.048°C/cm (approach to linearity)
Mean Temperature: -
Inflow Rate (Mean): 1.21 $mm^3 min^{-1}$
Outflow Rate (Mean): 2.18×10^{-1} $mm^3 min^{-1}$

EXPERIMENT NO. 4B, CASTOR SILT LOAM

Time Interval (Min)	Temperature Gradient (^{o}C)					Meniscus* (Distance travelled, mm)		Cumulative Flow (mm^3)	
	T_1	T_2	T_3	T_4	T_5	Inflow (-ve)	Outflow (+ve)	Inflow (-ve)	Outflow (+ve)
1050-1080	-0.500/ -0.500	-0.445/ -0.445	-0.325/ -0.325	-0.235/ -0.235	-0.200/ -0.205	0.0	3.0	0.00	0.59
1080-1110	-0.500	-0.440	-0.325	-0.235	-0.200	0.0	2.5	0.00	1.08
1110-1140	-0.505	-0.445	-0.325	-0.235	-0.205	0.5	1.5	0.10	1.37
1140-1170	-0.500	-0.445	-0.325	-0.235	-0.200	0.0	3.0	0.10	1.96
1170-1200	-0.500	-0.445	-0.325	-0.235	-0.200	0.0	2.5	0.10	2.45
1200-1230	-0.500	-0.440	-0.325	-0.235	-0.205	0.0	0.5	0.10	2.55
1230-1260	-0.505	-0.445	-0.325	-0.235	-0.205	+0.5	1.0	0.00	2.75
1260-1290	-0.500	-0.445	-0.325	-0.235	-0.205	0.0	1.0	0.00	2.95
1290-1320	-0.505	-0.440	-0.325	-0.235	-0.205	0.0	2.5	0.00	3.44
1320-1350	-0.505	-0.440	-0.325	-0.235	-0.200	0.0	3.5	0.00	4.12
1350-1380	-0.500	-0.445	-0.325	-0.235	-0.200	0.0	1.0	0.00	4.32
1380-1410	-0.500	-0.440	-0.325	-0.235	-0.200	0.0	6.5	0.00	5.60

*Radius of capillary tube = 0.025 cm

Initial Water Content: 41.33%
Temperature Gradient: $0.048^{o}C/cm$
Mean Temperature: $-0.350^{o}C$
Inflow Rate (Mean): 0.00 $mm^3 min^{-1}$
Outflow Rate (Mean): 1.55×10^{-2} $mm^3 min^{-1}$

EXPERIMENT NO. 4C, CASTOR SILT LOAM

Time Interval (Min)	Temperature Gradient (^{o}C)					Meniscus* (Distance travelled, mm)		Cumulative Flow (mm^3)	
	T_1	T_2	T_3	T_4	T_5	Inflow (-ve)	Outflow (+ve)	Inflow (-ve)	Outflow (+ve)
1440-1470	-0.600/ -0.600	-0.480/ -0.495	-0.340/ -0.355	-0.240/ -0.255	-0.205/ -0.200	+12.0	16.5	+2.36	3.24
1470-1500	-0.600	-0.505	-0.360	-0.255	-0.200	+7.5	13.0	+3.83	5.79
1500-1530	-0.600	-0.505	-0.365	-0.260	-0.205	+0.5	16.0	+3.93	8.94
1530-1560	-0.600	-0.505	-0.370	-0.265	-0.200	+1.5	2.5	+4.22	9.43
1560-1590	-0.600	-0.505	-0.370	-0.265	-0.200	+0.5	5.0	+4.32	10.41
1590-1620	-0.600	-0.505	-0.370	-0.265	-0.200	+0.5	4.5	+4.42	11.29
1620-1650	-0.600	-0.505	-0.370	-0.265	-0.200	+0.5	2.5	+4.52	11.78
1650-1680	-0.600	-0.510	-0.370	-0.265	-0.200	+0.5	0.5	+4.62	11.88
1680-1710	-0.605	-0.510	-0.370	-0.265	-0.205	0.5	3.0	+4.52	12.47
1710-1740	-0.600	-0.505	-0.370	-0.265	-0.200	0.0	0.5	+4.52	12.57
1740-1770	-0.600	-0.510	-0.370	-0.265	-0.200	0.0	0.0	+4.52	12.57
1770-1800	-0.600	-0.505	-0.370	-0.265	-0.200	0.0	1.5	+4.52	12.86

*Radius of capillary tube 0.025 cm

Initial Water Content: 41.33%
Temperature Gradient: $0.064^{o}C/cm$ (approach to linearity)
Mean Temperature: -
Inflow Rate (Mean): $+1.25 \times 10^{-2}$ $mm^3 min^{-1}$
Outflow Rate (Mean): 3.57×10^{-2} $mm^3 min^{-1}$

EXPERIMENT NO. 4D, CASTOR SILT LOAM

Time Interval (Min)	Temperature Gradient (^{o}C)					Meniscus* (Distance travelled, mm)		Cumulative Flow (mm^3)	
	T_1	T_2	T_3	T_4	T_5	Inflow (-ve)	Outflow (+ve)	Inflow (-ve)	Outflow (+ve)
2490-2520	-0.600/ -0.600	-0.510/ -0.510	-0.370/ -0.370	-0.265/ -0.265	-0.200/ -0.200	0.5	1.5	0.10	0.29
2520-2550	-0.600	-0.510	-0.370	-0.265	-0.205	0.0	3.0	0.10	0.88
2550-2580	-0.600	-0.505	-0.370	-0.265	-0.205	0.5	6.0	0.20	2.06
2580-2610	-0.600	-0.505	-0.375	-0.265	-0.200	+0.5	2.5	0.10	2.55
2610-2640	-0.600	-0.510	-0.370	-0.265	-0.205	0.0	4.0	0.10	3.34
2640-2670	-0.605	-0.510	-0.375	-0.265	-0.205	0.0	1.0	0.10	3.53
2670-2700	-0.605	-0.515	-0.375	-0.265	-0.200	0.5	2.0	0.20	3.93
2700-2730	-0.600	-0.510	-0.375	-0.265	-0.200	1.0	13.0	0.39	6.48
2730-2760	-0.605	-0.510	-0.370	-0.265	-0.200	0.0	2.5	0.39	6.97
2760-2790	-0.600	-0.510	-0.370	-0.265	-0.200	0.0	2.0	0.39	7.36
2790-2820	-0.600	-0.510	-0.370	-0.265	-0.200	0.0	6.5	0.39	8.64
2820-2850	-0.600	-0.510	-0.370	-0.265	-0.200	0.0	2.0	0.39	9.03

*Radius of capillary tube = 0.025 cm

Initial Water Content: 41.33%
Temperature Gradient: $0.064^{o}c/cm$
Mean Temperature: $-0.400^{o}C$
Inflow Rate (Mean): 1.09×10^{-3} $mm^3 min^{-1}$
Outflow Rate (Mean): 2.51×10^{-2} $mm^3 min^{-1}$

EXPERIMENT NO. 5A, CASTOR SILT LOAM
(Supercooled Water in Reservoirs)

Time Interval (Min)	Temperature Gradient (^{o}C)					Meniscus* (Distance travelled, mm)		Cumulative Flow (mm^3)	
	T_1	T_2	T_3	T_4	T_5	Inflow (-ve)	Outflow (+ve)	Inflow (-ve)	Outflow (+ve)
4290-4320	-0.305/ -0.300	-0.200/ -0.210	-0.135/ -0.135	-0.090/ -0.085	-0.105/ -0.095	+169.0	-172.0	+19.05	-16.69
4320-4350	-0.305	-0.215	-0.135	-0.090	-0.100	+51.5	-49.5	+52.24	-50.47
4350-4380	-0.300	-0.220	-0.140	-0.090	-0.095	+111.5	-138.5	+62.35	-60.19
4380-4410	-0.300	-0.220	-0.140	-0.090	-0.095	+137.0	-131.0	+84.25	-87.39
4410-4440	-0.300	-0.225	-0.140	-0.090	-0.095	+137.5	-131.0	+111.15	-113.11
4440-4470	-0.300	-0.230	-0.145	-0.090	-0.095	+157.0	-68.5	+138.15	-138.84
4470-4500	-0.305	-0.230	-0.145	-0.090	-0.105	+124.0	-101.0	+168.90	-152.29
4500-4530	-0.300	-0.230	-0.150	-0.090	-0.100	+30.0	-109.0	+193.31	-172.12
4530-4560	-0.300	-0.235	-0.155	-0.090	-0.105	+176.0	-115.5	+199.22	-193.53
4560-4590	-0.305	-0.240	-0.155	-0.095	-0.105	+148.5	-106.0	+233.78	-216.21
4590-4620	-0.300	-0.240	-0.155	-0.095	-0.100	+140.5	-15.0	+262.95	-237.03
4620-4650	-0.305	-0.245	-0.160	-0.095	-0.105	+96.0	-102.0	+290.54	-239.97

*Radius of capillary tube = 0.025 cm

Initial Water Content: 43.78%
Temperature Gradient: $0.032^{o}C/cm$
Mean Temperature: $-0.200^{o}C$
Inflow Rate (Mean): $+7.93 \times 10^{-1}\ mm^3 min^{-1}$
Outflow Rate (Mean): $-6.67 \times 10^{-1}\ mm^3 min^{-1}$

EXPERIMENT NO. 5B, CASTOR SILT LOAM
(Supercooled Water in Reservoirs)

Time Interval (Min)	Temperature Gradient (^{o}C)					Meniscus* (Distance travelled, mm)		Cumulative Flow (mm^3)	
	T_1	T_2	T_3	T_4	T_5	Inflow (-ve)	Outflow (+ve)	Inflow (-ve)	Outflow (+ve)
5370-5400	-0.300/ -0.300	-0.215/ -0.230	-0.140/ -0.155	-0.080/ -0.090	-0.100/ -0.100	+51.0	1.0	+10.02	0.20
5400-5430	-0.310	-0.255	-0.175	-0.105	-0.105	+93.5	-4.0	+28.38	-0.59
5430-5460	-0.300	-0.265	-0.185	-0.110	-0.100	+99.5	-31.0	+47.92	-6.68
5460-5490	-0.305	-0.265	-0.185	-0.115	-0.105	+91.5	-65.0	+65.88	-19.44
5490-5520	-0.290	-0.250	-0.170	-0.105	-0.095	+68.5	-71.5	+79.34	-33.48
5520-5550	-0.295	-0.250	-0.175	-0.105	-0.105	+69.5	-125.5	+92.98	-58.13
5550-5580	-0.300	-0.260	-0.185	-0.115	-0.105	+97.0	-1.0	+112.03	-58.32
5580-5610	-0.305	-0.270	-0.185	-0.115	-0.105	+16.5	-8.5	+115.27	-59.99
5610-5640	-0.300	-0.260	-0.185	-0.110	-0.105	+56.5	-22.5	+126.37	-64.41
5640-5670	-0.305	-0.260	-0.185	-0.115	-0.105	+64.0	-50.0	+138.94	-74.23
5670-5700	-0.295	-0.270	-0.190	-0.115	-0.095	+71.0	-58.0	+152.88	-85.62
5700-5730	-0.290	-0.255	-0.180	-0.110	-0.095	+60.5	-97.5	+164.76	-104.77

*Radius of capillary tube 0.025 cm

Initial Water Content: 43.78%
Temperature Gradient: $0.032^{o}C/cm$
Mean Temperature: $-0.200^{o}C$
Inflow Rate (Mean): $+4.58 \times 10^{-1}\ mm^3 min^{-1}$
Outflow Rate (Mean): $-2.91 \times 10^{-1} mm^3 min^{-1}$

EXPERIMENT NO. 6A, SLIMS VALLEY SILT
(Supercooled Water in Reservoirs)

Time Interval (Min)	Temperature Gradient (^{o}C)					Meniscus* (Distance travelled, mm)		Cumulative Flow (mm^3)	
	T_1	T_2	T_3	T_4	T_5	Inflow (-ve)	Outflow (+ve)	Inflow (-ve)	Outflow (+ve)
1320-1350	-0.095/ -0.095	-0.075/ -0.075	-0.085/ -0.085	-0.065/ -0.065	-0.100/ -0.100	+0.5	-0.5	+0.10	-0.10
1350-1380	-0.100	-0.075	-0.085	-0.065	-0.100	0.0	-79.5	+0.10	-15.71
1380-1410	-0.100	-0.080	-0.085	-0.065	-0.095	0.0	-2.5	+0.10	-16.20
1410-1440	-0.100	-0.080	-0.085	-0.065	-0.100	+3.0	-1.0	+0.69	-16.40
1440-1470	-0.085	-0.080	-0.085	-0.065	-0.100	+1.0	0.0	+0.88	-16.40
1470-1500	-0.100	-0.080	-0.085	-0.070	-0.095	+6.0	-0.5	+2.06	-16.49
1500-1530	-0.100	-0.090	-0.110	-0.075	-0.095	+3.5	-2.0	+2.75	-16.89
1530-1560	-0.100	-0.085	-0.105	-0.090	-0.100	+3.5	-62.0	+3.44	-29.10
1560-1590	-0.105	-0.080	-0.090	-0.070	-0.095	0.0	-60.5	+3.44	-40.94
1590-1620	-0.100	-0.085	-0.085	-0.065	-0.100	0.0	-24.0	+3.44	-45.65
1620-1650	-0.095	-0.085	-0.085	-0.065	-0.100	2.0	-47.7	+3.04	-54.98
1650-1680	-0.100	-0.085	-0.090	-0.070	-0.100	0.0	0.0	+3.04	-54.98

*Radius of capillary tube = 0.025 cm

Initial Water Content: 29.92%
Temperature Gradient: $0.00^{o}C/cm$
Mean Temperature: $-0.100^{o}C$
Inflow Rate (Mean): $+8.44 \times 10^{-3}$ $mm^3 min^{-1}$
Outflow Rate (Mean): -1.15×10^{-1} $mm^3 min^{-1}$

EXPERIMENT NO. 6B, SLIMS VALLEY SILT
(Supercooled Water in Reservoirs)

Time Interval (Min)	Temperature Gradient (^{o}C)					Meniscus* (Distance travelled, mm)		Cumulative Flow (mm^3)	
	T_1	T_2	T_3	T_4	T_5	Inflow (-ve)	Outflow (+ve)	Inflow (-ve)	Outflow (+ve)
8310-8340	-0.200/ -0.205	-0.175/ -0.175	-0.165/ -0.170	-0.120/ -0.125	-0.100/ -0.105	+3.5	-0.5	+0.69	-0.10
8340-8370	-0.200	-0.160	-0.150	-0.105	-0.105	0.0	-2.5	+0.69	-0.59
8370-8400	-0.200	-0.160	-0.145	-0.105	-0.095	+48.5	-3.5	+10.21	0.10
8400-8430	-0.205	-0.175	-0.160	-0.115	-0.100	0.0	0.0	+10.21	0.10
8430-8460	-0.205	-0.175	-0.165	-0.125	-0.100	+1.0	0.0	+10.41	0.10
8460-8490	-0.205	-0.180	-0.175	-0.125	-0.100	0.0	-0.5	+10.41	0.00
8490-8520	-0.200	-0.165	-0.145	-0.105	-0.100	0.0	-4.0	+10.41	-0.79
8520-8550	-0.205	-0.175	-0.160	-0.115	-0.100	0.0	0.0	+10.41	-0.79
8550-8580	-0.205	-0.180	-0.170	-0.125	-0.105	1.0	-0.5	+10.21	-0.88
8580-8610	-0.205	-0.180	-0.170	-0.125	-0.105	0.0	-9.5	+10.21	-2.75
8610-8640	-0.200	-0.165	-0.155	-0.110	-0.095	0.5	-7.0	+10.11	-4.12
8640-8670	-0.200	-0.170	-0.160	-0.120	-0.100	0.0	-5.5	+10.11	-5.20

*Radius of capillary tube = 0.025 cm

Initial Water Content: 29.92%
Temperature Gradient: $0.016^{o}C/cm$
Mean Temperature: $-0.150^{o}C$
Inflow Rate (Mean): $+2.02 \times 10^{-2}$ $mm^3 min^{-1}$, for period 8310-8790 min
Outflow Rate (Mean): -2.67×10^{-2} $mm^3 min^{-1}$, for period 8310-8790 min